Thermodynamics and superfluid density in BCS-BEC crossover with and without population imbalance

Yan He, Chih-Chun Chien, Qijin Chen, and K. Levin
James Franck Institute and Department of Physics, University of Chicago, Chicago, Illinois 60637, USA
(Received 12 July 2007; published 17 December 2007)

We address the thermodynamics, density profiles, and superfluid density of trapped fermions undergoing BCS-BEC crossover. We consider the case of zero and finite population imbalance and apply the local density approximation (LDA) to include the trap potential. Our approach represents a fully self-consistent treatment of "pseudogap effects." These effects reflect the distinction between the pair formation temperature T^* and the pair condensation temperature T_c. As a natural corollary, this temperature difference must be accommodated in the fermionic excitation spectrum $E_{\mathbf{k}}$ to reflect the fact that fermions are paired at and above T_c. It is precisely this natural corollary which has been omitted from all other many body approaches in the literature. At a formal level, we show how enforcing this corollary implies that pairing fluctuation or self-energy contributions enter into *both* the gap and the number equations; this is necessary in order to be consistent with a generalized Ward identity. At a less formal level, we demonstrate that we obtain physical results for the superfluid density $n_s(T)$ at all temperatures. In contrast, previous work in the literature has led to nonmonotonic, or multivalued or discontinuous behavior for $n_s(T)$. Because it reflects the essence of the superfluid state, *we view the superfluid density as a critical measure of the physicality of a given crossover theory*. In a similarly unique fashion, we emphasize that in order to properly address thermodynamic properties of a trapped Fermi gas, a necessary first step is to demonstrate that the particle density profiles are consistent with experiment. Without a careful incorporation of the distinction between the pairing gap and the order parameter, the LDA-derived density profiles (of the unpolarized gas) tend to exhibit sharp features at the condensate edge, which are never seen experimentally in the crossover regime. The lack of demonstrable consistency between theoretical and experimental density profiles, along with problematic behavior found for the superfluid density, casts doubt on previous claims in the literature concerning quantitative agreement between thermodynamical calculations and experiment.

DOI: 10.1103/PhysRevB.76.224516 PACS number(s): 03.75.Hh, 03.75.Ss, 74.20.−z

I. INTRODUCTION

There has been a resurgence of interest in studies of the crossover between the usual BCS form of fermionic superfluidity and that associated with Bose Einstein condensation (BEC). This is due, in part, to the widespread pseudogap phenomena which have been observed in high temperature superconductors in conjunction with the small pair size. The latter, in particular, was argued by Leggett to be a rationale[1] for treating the cuprates as midway between BCS and BEC. Others have argued[2–4] that the cuprate pseudogap can be understood as arising from preformed pairs which form due to the stronger-than-BCS attraction. Additional reasons for the interest in BCS-BEC crossover stem from the precise realization of this scenario in ultracold trapped Fermi gases,[3,5–8] where the attractive interaction can be continuously tuned from weak to strong via a Feshbach resonance in the presence of a magnetic field. A final rationale for interest in this problem stems from the fact that BCS theory is the prototype for successful theories in condensed matter physics; and we now have come to realize that this is a very special case of a much more general class of superfluidity.

BCS-BEC crossover theory is based on the observation[9,10] that the usual BCS ground state wave function $\Psi_0=\Pi_{\mathbf{k}}(u_{\mathbf{k}}+v_{\mathbf{k}}c^{\dagger}_{\mathbf{k},\uparrow}c^{\dagger}_{-\mathbf{k},\downarrow})|0\rangle$ (where $c^{\dagger}_{\mathbf{k},\sigma}$ and $c_{\mathbf{k},\sigma}$ are the creation and annihilation operators for fermions of momentum $\mathbf{k}$ and spin $\sigma=\uparrow,\downarrow$) is far more general than was initially appreciated. If one tunes the attractive interaction from weak to strong, along with a self-consistent determination of the variational parameters $v_{\mathbf{k}}$ and $u_{\mathbf{k}}$ the chemical potential passes from positive to negative and the system crosses continuously from BCS to BEC. The vast majority (with the possible exception of the high-T_c cuprates) of metallic superconductors are associated with weak attraction and large pair size. Thus, this more generalized form of BCS theory was never fully characterized or exploited until recently. There are a number of different versions of BCS-BEC crossover theory. Each can be represented by a selected class of many-body Feynman diagrams, often further simplified by various essential or nonessential approximations. There is no controlled small parameter and thus the selection process is based on highly variable criteria. For the most part the success or failure of a particular rendition is evaluated by comparing one or a set of numbers with experiment.

It is the goal of the present paper to discuss a criteria set for evaluating BCS-BEC crossover theories which captures the crucial physics, rather than the detailed numerics. We apply these criteria successfully to one particular version of BCS-BEC crossover theory which builds on the above ground state. In this context we address a wide range of physical phenomena. These include local density approximation (LDA)–computed density profiles, thermodynamical properties and superfluid density with application to polarized as well as unpolarized gases. *It is our philosophy that appropriate tests of the theory should relate to how qualitatively sound it is before assessing it in quantitative detail.*

Detailed quantitative tests are essential but if the qualitative physics is not satisfactory, quantitative comparisons cannot be meaningful.

Four important and inter-related physical properties are emphasized here. (i) There must be a self-consistent treatment of "pseudogap" effects.[4] As a consequence of the fact that the pairing onset temperature T^* is different[11,12] from the condensation temperature T_c, the fermionic spectrum, $E_{\mathbf{k}}$ must necessarily reflect the formation of these pairs. To accommodate the pseudogap, $E_{\mathbf{k}}$ *cannot* assume the strict BCS form which has a vanishing excitation gap at and above T_c. Everywhere in the literature it is assumed that $E_{\mathbf{k}}$ is of the strict BCS form, except in our own work and briefly in Ref. 13. (ii) The theory must yield a self-consistent description of the superfluid density $n_s(T)$ from zero to T_c. The quantity $n_s(T)$ should be single valued, monotonic,[14] and disappear at the same T_c one computes from the normal state instability. Importantly, $n_s(T)$ is at the heart of a proper description of the superfluid phase. (iii) The behavior of the density profiles, which are the basis for computing thermodynamical properties of trapped gases, must be compatible with experimental measurements. Near and at unitarity, and in the absence of population imbalance, they are relatively smooth and featureless (unlike a true BEC where there is clear bimodality). This can present a challenge for theories which do not accommodate pseudogap effects and which then deduce sharp features at the condensate edge for an unpolarized gas. (iv) The thermodynamic potential Ω should be variationally consistent with the gap and number equations. If, as usually assumed, pairing fluctuations enter into the number equation but not the gap equation, then these equations are generally not variationally derivable from Ω. Moreover, the thermodynamic potential should satisfy appropriate Maxwell relations and at unitarity be compatible with the constraint[15,16] relating the pressure p to the energy, E: $p=\frac{2}{3}E$.

There has been widespread discussion about the role of collective modes in the thermodynamics of fermionic superfluids. And this has become, in some instances, a basis for additional evaluation criteria of a given BCS-BEC crossover theory. Because the Fermi gases represent neutral superfluids with low lying collective modes, one might have expected these modes to be more important than in charged superconductors. Nevertheless, the BCS wave function and its associated finite temperature behavior is well known to work equally well for charged superconductors and neutral superfluids such as helium-3. In strict BCS theory thermodynamical properties are governed only by fermionic excitations. This applies as well to the superfluid density (in the transverse gauge). Collective modes are important in strict BCS theory primarily to establish that $n_s(T)$ is properly gauge invariant.

One can argue[17] that collective modes should enter thermodynamics as the pairing attraction becomes progressively stronger. The role of these modes at unitarity is currently unresolved. In the Bogoliubov description of a true Bose superfluid there is a coupling between the pair excitations and the collective modes, which results from interboson interactions. Thus it is reasonable to expect that the collective modes are important for thermodynamical properties in the BEC regime. At the level of the simple mean BCS-Leggett wave function we find that, just as in strict BCS theory, the collective modes do not couple to the pair excitations; this leads to a $q^2/2M^*$ form of the pair dispersion. The low-lying collective mode dispersion is,[18] of course, linear in q. All interboson effects are treated in a mean field sense and enter to renormalize the effective pair mass M^*. To arrive at a theory more closely analogous to Bogoliubov theory, one needs to add additional terms to the ground state wave function—consisting of four and six creation operators[19] in the deep BEC. The complexity becomes even greater in the unitary regime, and there is, in our opinion, no clear indication one way or the other on how the pair excitations and collective modes couple.

Our rationale for considering the simplest ground state wave function (which minimizes this coupling between the collective and pair excitation modes) is as follows. It is the basis for zero temperature Bogoliubov–de Gennes (BdG) approaches which have been widely applied to the crossover problem. It is the basis for a $T=0$ Gross-Pitaevskii description in the far BEC regime.[20] It is the basis for the bulk of the work on population imbalanced gases.[21,22] At unitarity the universality relation[15,16] between pressure and energy holds—separately for the fermionic contribution (which is of the usual BCS form with an excitation gap distinct from the order parameter) and for the bosonic term, due to the q^2 form of the pair dispersion. Finally, this wave function is simple and accessible. Thus it seems reasonable to begin by addressing the finite T physics which is associated with this ground state, in a systematic way.

The remainder of this paper presents first the theoretical framework for the principal self-consistent equations describing the total excitation gap, the order parameter, and the number equation or fermionic chemical potential. The consequences for thermodynamics, LDA-computed density profiles and the superfluid density are then presented in separate sections, along with numerically obtained results for each property. We discuss these properties at the qualitative as well as semi-quantitative level, in the context of comparison with experiment. In the Conclusions section, we present a summary of the strengths and weaknesses of the present scheme.

To make this paper more self-contained and, thus, easier to read, we recapitulate in Secs. II–V some aspects of a theoretical framework which has appeared in previous papers. More details of the theoretical formalism can be found in Ref. 3 (which addresses the two-channel model in the absence of population imbalance) and Ref. 23 (which addresses the one-channel model in the presence of population imbalance). At the same time, we compare our theory with alternative approaches in the literature.

II. THEORETICAL BACKGROUND

A. Pseudogap effects in BCS-BEC crossover

While the subject of BCS-BEC crossover began with the seminal $T=0$ work by Eagles [9] and Leggett,[10] a discussion of superfluidity beyond the ground state was first introduced into the literature by Nozières and Schmitt-Rink.[17] Randeria and co-workers reformulated this approach[17] and moreover, raised the interesting possibility that crossover physics might be relevant to high temperature superconductors[12]. Subsequently other workers have applied this picture to the high-T_c cuprates[24–27] and ultracold Fermi gases[28,29] as well as formulated alternative schemes[30,31] for addressing $T \neq 0$.

The introduction of pseudogap effects into a treatment of BCS-BEC crossover was a crucial next step. It was first recognized that one should distinguish the pair formation temperature T^* from the condensation temperature T_c.[11,12] That the magnetic properties of the normal phase in the temperature regime between T_c and T^* would be anomalous was pointed out on the basis of numerical calculations, on a two dimensional lattice. Here it was found that the spin susceptibility was depressed at low temperatures[32] and this depression was associated with a "spin gap" which is to be distinguished from a pseudogap. Indeed, in reviewing this earlier work,[2] it was argued that "there is no pseudogap in the charge channel."

The fact that BCS-BEC crossover theory was, indeed, associated with a pseudogap, thus, required further analysis and calculations. Using the formalism of the present paper, subsequent, theoretical studies of the spectral function (both above[33] and below[34] T_c) and the superfluid density[35] showed that, despite earlier claims,[2] a normal state pairing gap appeared in *both* the spin and charge channels and, furthermore, affected the behavior below T_c as well[35] as above.

At roughly the same time, other approaches to BCS-BEC crossover reported a four excitation branch structure[36,37] in the spectral function, not compatible with the expected pseudogap description, which should exhibit precursor superconductivity effects. In the standard pseudogap picture,[3,33,38] there would be two peaks in the normal state spectral function, rather than four; in the simplest terms, this spectral function represents a broadened version of its below T_c, BCS counterpart. Indeed the observation of a two peaked spectral function in the normal state[39,40] is now taken as some of the strongest evidence in hand for a pseudogap phase in the cuprate superconductors, although there is no consensus about whether its origin lies in BCS-BEC crossover. It should be noted that the pseudogap and superfluid order parameter have the same d-wave symmetry,[41] as is to be expected in crossover theory. More recently, alternative approaches to BCS-BEC crossover[27] have reached the same conclusion as in Ref. 33, that BCS-BEC crossover does lead to spectral functions with a normal state gap and (for the d-wave case) with general behavior not so different from that observed in the high temperature superconductors.[24,38]

Finally, we make note of those papers where the concept of pseudogap effects was introduced into studies of the ultracold gases. Two groups[42,43] more or less simultaneously called attention to the presence of a pseudogap in a unitary Fermi gas and noted that (unlike in strict BCS theory) the existence of a pairing gap could not be used to infer the presence of superfluidity. The most notable experimental consequences for the gases[4] lay in RF spectroscopy experiments[44] and their theory,[45–47] as well as in thermodynamics.[48] Indeed, in Refs. 45 and 46, the authors made use of the formalism of the present paper and, in the latter reference, were the first to incorporate trap effects within the LDA. The present formalism has also been used to address trapped polarized gases first in Ref. 49.

B. Bogoliubov–de Gennes approaches to crossover

There has been a fairly extensive literature on applications of Bogoliubov–de Gennes (BdG) theory to ultracold Fermi gases. Like the crossover theory of the present paper, this approach is based on the same BCS-Leggett form for the ground state at $T=0$. (In a strict sense this wave function applies only to a homogeneous Fermi gas in the absence of population imbalance). Most of the attention has focused on the case of an imbalanced population of the two fermion states.[22,50] An important advantage of the BdG theory is that it can address the effects of the trap without the necessity for introducing the LDA approximation. Furthermore, exotic phases such as the Larkin-Ovchinnikov-Fulde-Ferrell (LOFF) states[51] will naturally emerge whenever they are appropriate. The disadvantage of this BdG scheme is that it does not incorporate pseudogap effects and so is restricted to strictly $T=0$, and it does not easily address the conditions under which stability relative to other phases (e.g., phase separation) must be assessed.

In this context and in contrast to LDA-based schemes, BdG-based calculations[21,22] suggest that the population imbalanced ground state is not phase separated at unitarity, but rather corresponds to a LOFF phase.[51] By contrast, experiments from two (major) experimental groups seem to support phase separation.[52,53] We have conducted a finite temperature study (importantly including noncondensed pairs) of the simplest such state[54] which suggests that this oscillatory order parameter phase rapidly becomes unstable with increasing temperature. Because it is not sufficiently robust and because it is not seen experimentally, we argue that the LOFF phase found in BdG-based schemes may reflect inadequacies of this approach. At the very least, in the absence of evidence to support an oscillatory order parameter, BdG theory should not preempt consideration of the LDA-based schemes which we address in the present paper. Both approaches should be actively pursued.

C. Pair fluctuation approaches to crossover

In this section we discuss the present T-matrix based scheme for BCS-BEC crossover, as well as compare it with alternative approaches including that of Nozières and Schmitt-Rink.[17] The Hamiltonian for BCS-BEC crossover can be described by a one-channel model. In this paper, we address primarily a short range s-wave pairing interaction, which is often simplified as a contact potential $U\delta(\mathbf{x}-\mathbf{x}')$, where $U<0$. This Hamiltonian has been known to provide a good description for the crossover in atomic Fermi gases which have very wide Feshbach resonances, such as ^{40}K and ^{6}Li. The details are presented elsewhere.[3]

Within a T-matrix scheme one considers the coupled equations between the particles (with propagator G) and the pairs [which can be represented by the T-matrix $t(Q)$] and drops all higher order terms. Without taking higher order Green's functions into account, the pairs interact indirectly via the fermions, in an averaged or mean field sense. The propagator for the noncondensed pairs is given by

$$t_{\mathrm{pg}}^{-1}(Q) = U^{-1} + \chi(Q), \tag{1}$$

where U is the attractive coupling constant in the Hamiltonian and χ is the pair susceptibility. The function $\chi(Q)$ is the most fundamental quantity in T-matrix approaches. It is given by the product of dressed and bare Green's functions in various combinations. One could, in principle, have considered two bare Green's functions or two fully dressed Green's functions. Here, we follow the work of Ref. 55. These authors systematically studied the equations of motion for the Green's functions associated with the usual many body Hamiltonian for superfluidity and deduced that the only satisfactory truncation procedure for these equations involves a T-matrix with one dressed and one bare Green's function, (and with a bare Green's function in the self energy). This asymmetric combination in the T-matrix is a general, and inevitable, consequence of an equations of motion procedure; it is not an ad hoc assumption and more details of its derivation can be found in Ref. 56.

In this approach, the pair susceptibility is then

$$\chi(Q) = \sum_K G_0(Q-K)G(K), \tag{2}$$

where $Q=(i\Omega_l,\mathbf{q})$, and G and G_0 are the full and bare Green's functions, respectively. Here $G_0^{-1}(K)=i\omega_n-\xi_{\mathbf{k}}$, $\xi_{\mathbf{k}}=\epsilon_{\mathbf{k}}-\mu$, $\epsilon_{\mathbf{k}}=\hbar^2k^2/2m$ is the kinetic energy of fermions, and μ is the fermionic chemical potential. Throughout this paper, we take $\hbar=1$, $k_B=1$, and use the four-vector notation $K\equiv(i\omega_n,\mathbf{k})$, $Q\equiv(i\Omega_l,\mathbf{q})$, $\Sigma_K\equiv T\Sigma_n\Sigma_{\mathbf{k}}$, etc., where $\omega_n=(2n+1)\pi T$ and $\Omega_l=2l\pi T$ are the standard odd and even Matsubara frequencies[57](where n and l are integers).

The one-particle Green's function is

$$G^{-1}(K) = i\omega_n - \xi_{\mathbf{k}} - \Sigma(K), \tag{3}$$

where

$$\Sigma(K) = \sum_Q t(Q)G_0(Q-K). \tag{4}$$

More generally, either G_0 or the fully dressed G is introduced into $\Sigma(K)$, according to the chosen T-matrix scheme. Finally, in terms of Green's functions, we readily arrive at the number equation: $n=\Sigma_{K,\sigma}G_\sigma(K)$.

Because of interest from high temperature superconductivity, alternate schemes, which involve only dressed Green's functions have been rather widely studied.[36,37,58] In one alternative,[59] one constructs a thermodynamical potential based on a chosen self-energy. Here there is some similarity to that T-matrix scheme which involves G only. One variant of this "conserving approximation" is known as the fluctuation exchange approximation (FLEX) which has been primarily applied to the normal state.[60] In addition to the particle-particle ladder diagrams which are crucial to superfluidity it also includes less critical diagrams in the particle-hole channel; the latter can be viewed as introducing spin correlation effects. Since it involves only dressed Green's functions, one evident advantage of this approach is that it is Φ-derivable[61] and thus referred to as "conserving." This implies that because it is based on an analytical expression for the thermodynamical potential, thermodynamical quantities obtained by derivatives of the free energy are identical to those computed directly from the single particle Green's function.

For a variety of reasons this FLEX scheme, as applied to superfluids and superconductors, has been found to be problematic. The earliest critique of the GG, T-matrix scheme is in Ref. 55. The authors noted that using two dressed Green's functions "could be rejected by means of a variational principle." They also observed that there would be an unphysical consequence: A low T specific heat which contained a contribution proportional to T^2. In a related fashion it appears that the FLEX or GG, T-matrix scheme is *not* demonstrably consistent with the Hamiltonian-based equations of motion. There is also concern that considering only dressed fermion propagators, G, may lead to double counting of Feynman diagrams. Vilk *et al.*[62] noted that the FLEX scheme will not produce a proper pseudogap, due to the "inconsistent treatment of vertex corrections in the expression for the self energy."

By dropping the nondominant particle-hole diagrams, others have found a more analytically tractable scheme.[63] However, this scheme fails to yield back BCS-like spectral properties which would be anticipated above T_c in a BCS-BEC crossover scenario. Among the unusual features found is the four excitation branch structure,[36,37] discussed above. More recently, the authors of Ref. 64 applied a related conserving approximation below T_c. They did not consider particle-hole diagrams, but included in the particle-particle channel a "twisted" ladder diagram. These authors found that there was a discontinuity in the transition temperature calculated relative to that computed[58] above T_c. They, then, inferred that at unitarity there is a first order phase transition, which has not been experimentally observed.

In the NSR scheme, which is, perhaps, the most widely applied of all pair fluctuation theories,[12] one uses two bare Green's functions in $\chi(Q)$ in the normal state. Within this NSR approach, the results are generally extended below T_c by introducing[43] into $\chi(Q)$ the diagonal and off-diagonal forms of the Nambu-Gor'kov Greens functions. At the outset, the fermionic excitation spectrum $E_{\mathbf{k}}=\sqrt{\xi_{\mathbf{k}}^2+\Delta_{\mathrm{sc}}^2}$ involves only the superfluid order parameter, Δ_{sc}, so that the fermions are treated as gapless at and above T_c, despite the fact that there is an expected "pseudogap" associated with the pairing onset temperature T^*. The authors[17] suggested that pair fluctuations should enter into the number equation, but approximated their form based on only[65] the leading contribution in the Dyson series. This approximate form was introduced via a pair fluctuation contribution to the thermodynamical potential Ω. A more systematic approach, which is based on a full Dyson resummation leads to a form equivalent to Eq. (4), with a bare $\chi_0(Q)=\Sigma_K G_0(K)G_0(Q-K)$, as was first pointed out in Ref. 65. This more complete scheme was implemented in Ref.43.

Another important aspect of the NSR scheme should be noted. Because the pairing fluctuation contributions do not enter into the gap equation, *the gap equation cannot be determined from a variational condition on the thermodynamic potential*. To address this shortcoming, a rather different alternative to the approximated number equation of Ref. 17 was recently introduced in Refs. 66 and 67. These authors argued one should compensate for the fact that $d\Omega/d\Delta_{sc} \neq 0$ by adding a new term (deriving from this discrepancy) to the number equation. We view this latter alternative as even more problematic since it builds on inconsistencies within the NSR approach in *both* the gap and the number equation. By far the most complete study of the NSR based theory for crossover was summarized in Ref. 13. By systematically introducing a series of improved approximations, the authors ultimately noted that one must incorporate pairing fluctuation corrections into the gap as well as the number equation.

It should be stressed that (with or without the approximate form for the number equation) *the NSR scheme at $T\neq 0$ was not designed to be consistent with the simple BCS-Leggett ground state, which they also discussed at length*. This observation was implicitly made elsewhere[68] in the literature and can be verified by comparing the ground state density profiles based on the NSR scheme with those obtained in the Leggett mean field theory.[68] It should also be stressed that T-matrix theories do not incorporate a direct pair-pair interaction; rather the pairs interact in an average or mean field sense. If one tries to extract the effective pairing interaction from *any* T-matrix theory, the absence of coupling to higher order Green's functions will lead to a simple factor of 2 relating the interboson and interfermion scattering lengths. More exact calculations of this ratio lead to a factor of 0.6.[19,69–72]

D. Present T-matrix scheme

We now show that one obtains consistent answers between T-matrix based approaches and the BCS-Leggett ground state equations, provided the pair susceptibility contains one bare and one dressed Green's function. Thus, for simplicity, we refer to the present approach as "GG_0 theory." Throughout this paper we will emphasize the strengths of the present T-matrix scheme which rest primarily on a consistent treatment of pseudogap effects in the gap and number equations. This, in turn, leads to physical behavior for the thermodynamics, the superfluid density and the density profiles at all temperatures. Finally, we note that the present T-matrix scheme is readily related to a previously studied[73] approach to fluctuations in low dimensional, but conventional superconductors. A weak coupling limit of this GG_0 approach is equivalent to Hartree approximated Ginzburg-Landau theory.[42]

We begin with the situation in which there is an equal spin mixture, and then generalize to the population imbalanced case. In the present formalism, for all $T\leq T_c$, the gap equation is associated with a BEC condition which requires that the pair chemical potential μ_{pair} vanish. We will show below that because of this vanishing of μ_{pair} at and below T_c, to a good approximation one can move G_0 outside the summation in Eq. (4). As a result the self energy is of the BCS-like form

$$\Sigma(K) = -\Delta^2 G_0(-K) = \frac{\Delta^2}{i\omega_n + \xi_{\mathbf{k}}}. \tag{5}$$

Thus

$$G^{-1}(K) = i\omega_n - \xi_{\mathbf{k}} - \frac{\Delta^2}{i\omega_n + \xi_{\mathbf{k}}}. \tag{6}$$

Now we are in a position to calculate the pair susceptibility at general Q, based on Eq. (2). After performing the Matsubara sum and analytically continuing to the real axis, $i\Omega_l \to \Omega + i0$) we find the relatively simple form

$$\chi(Q) = \sum_{\mathbf{k}} \left[\frac{1-f(E_{\mathbf{k}})-f(\xi_{\mathbf{k-q}})}{E_{\mathbf{k}}+\xi_{\mathbf{k-q}}-\Omega-i0^+} u_{\mathbf{k}}^2 - \frac{f(E_{\mathbf{k}})-f(\xi_{\mathbf{k-q}})}{E_{\mathbf{k}}-\xi_{\mathbf{k-q}}+\Omega+i0^+} v_{\mathbf{k}}^2 \right], \tag{7}$$

where $u_{\mathbf{k}}^2, v_{\mathbf{k}}^2 = (1\pm\xi_{\mathbf{k}}/E_{\mathbf{k}})/2$ are the usual coherence factors, and $f(x)$ is the Fermi distribution function. It follows that $\chi(0)$ is given by

$$\chi(0) = \sum_{\mathbf{k}} \frac{1-2f(E_{\mathbf{k}})}{2E_{\mathbf{k}}}. \tag{8}$$

The vanishing of μ_{pair} (or generalized Thouless criterion) then implies that

$$t_{pg}^{-1}(0) = U^{-1} + \chi(0) = 0, \quad T \leq T_c. \tag{9}$$

Substituting $\chi(0)$ into the above BEC condition, we obtain the familiar gap equation

$$0 = \frac{1}{U} + \sum_{\mathbf{k}} \frac{1-2f(E_{\mathbf{k}})}{2E_{\mathbf{k}}}. \tag{10}$$

Here $E_{\mathbf{k}} = \sqrt{\xi_{\mathbf{k}}^2 + \Delta^2}$, which contains the total excitation gap Δ instead of the order parameter Δ_{sc}. It should be noted that this BCS form for $E_{\mathbf{k}}$ is not imposed or forced, but rather it is a natural consequence of GG_0 theory.

The coupling constant U can be replaced in favor of the dimensionless parameter, $1/k_F a$, via the relationship $m/(4\pi a) = 1/U + \sum_{\mathbf{k}} (2\epsilon_{\mathbf{k}})^{-1}$, where a is the two-body s-wave scattering length, and k_F is the noninteracting Fermi wave vector for the same total number density. Therefore, the gap equation can be rewritten as

$$-\frac{m}{4\pi a} = \sum_{\mathbf{k}} \left[\frac{1-2f(E_{\mathbf{k}})}{2E_{\mathbf{k}}} - \frac{1}{2\epsilon_{\mathbf{k}}} \right]. \tag{11}$$

Here the "unitary scattering" limit corresponds to resonant scattering where $a\to\infty$. For atomic Fermi gases, this scattering length is tunable via a Feshbach resonance by application of a magnetic field and we say that we are on the BCS or BEC side of resonance, depending on whether the fields are higher or lower than the resonant field, or alternatively whether a is negative or positive, respectively.

Finally, inserting the self energy of Eq. (5), into the Green's function, it follows that the number equation is given by

$$n = 2\sum_{\mathbf{k}} [f(E_{\mathbf{k}}) u_{\mathbf{k}}^2 + f(-E_{\mathbf{k}}) v_{\mathbf{k}}^2], \tag{12}$$

thus demonstrating that both the number and gap equation [see Eq. (10)] are consistent with the ground state constraints in BCS-Leggett theory.

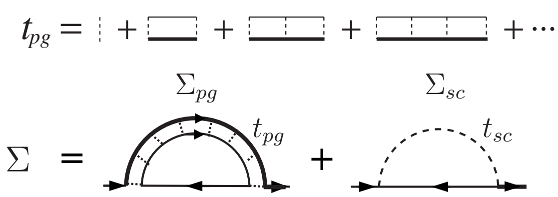

FIG. 1. T-matrix and self-energy diagrams for the present T-matrix scheme. The self-energy comes from contributions of both condensed (Σ_{sc}) and noncondensed (Σ_{pg}) pairs. Note that there is one dressed and full Green's function in the T-matrix. Here the T-matrix t_{pg} can be regarded effectively as the propagator for the noncondensed pairs.

Next we use this T-matrix scheme to derive Eq. (5) and separate the contribution from condensed and noncondensed pairs. The diagrammatic representation of our T-matrix scheme is shown in Fig. 1. The first line indicates the T-matrix, t_{pg}, and the second the total self-energy. The T-matrix can be effectively regarded as the propagator for noncondensed pairs. One can see throughout the combination of one dressed and one bare Green's function, as represented by the thick and thin lines. The self energy consists of two contributions from the noncondensed pairs or pseudogap (pg) and from the condensate (sc). There are, analogously, two contributions to the full T-matrix

$$t = t_{\text{pg}} + t_{\text{sc}}, \tag{13}$$

$$t_{\text{pg}}(Q) = \frac{U}{1 + U\chi(Q)}, \quad Q \neq 0, \tag{14}$$

$$t_{\text{sc}}(Q) = -\frac{\Delta_{\text{sc}}^2}{T}\delta(Q), \tag{15}$$

where we write $\Delta_{\text{sc}}=-U\Sigma_{\mathbf{k}}\langle c_{-\mathbf{k}\downarrow}c_{\mathbf{k}\uparrow}\rangle$. Similarly, we have for the fermion self-energy

$$\Sigma(K) = \Sigma_{\text{sc}}(K) + \Sigma_{\text{pg}}(K) = \sum_Q t(Q)G_0(Q-K). \tag{16}$$

We see at once that

$$\Sigma_{\text{sc}}(K) = \sum_Q t_{\text{sc}}(Q)G_0(Q-K) = -G_0(-K)\Delta_{\text{sc}}^2. \tag{17}$$

A vanishing chemical potential means that $t_{\text{pg}}(Q)$ diverges at $Q=0$ when $T \leq T_c$. Thus we approximate[74,75] Eq. (16) to yield

$$\Sigma(K) \approx -G_0(-K)\Delta^2, \tag{18}$$

where

$$\Delta^2(T) \equiv \Delta_{\text{sc}}^2(T) + \Delta_{\text{pg}}^2(T). \tag{19}$$

Under this approximation, now the total self-energy assumes the BCS form. The fact that Δ_{sc} and Δ_{pg} add to each other in quadrature lies in that their square are proportional to the density of condensed and noncondensed pairs, respectively. Importantly, we are led to identify the quantity Δ_{pg}

$$\Delta_{\text{pg}}^2 \equiv -\sum_{Q \neq 0} t_{\text{pg}}(Q). \tag{20}$$

Note that in the normal state (where μ_{pair} is nonzero), Eq. (18) is no longer a good approximation. We now have a closed set of equations for addressing the ordered phase. We show later how to extend this approach to temperatures somewhat above T_c, by self-consistently including a nonzero pair chemical potential. This is a necessary step in addressing a trap as well.[76]

The propagator for noncondensed pairs can now be quantified, using the self-consistently determined pair susceptibility. At small four-vector Q, we may expand the inverse of t_{pg}, after analytical continuation, to obtain

$$t_{\text{pg}}^{-1}(Q) \approx a_1\Omega^2 + Z\left(\Omega - \frac{q^2}{2M^*} + \mu_{\text{pair}} + i\Gamma_Q\right), \tag{21}$$

where below T_c the imaginary part $\Gamma_Q \to 0$ faster than q^2 as $q \to 0$. Because we are interested in the moderate and strong coupling cases, where the contribution of the $a_1\Omega^2$ term is small, we drop it in Eq. (21) so that

$$t_{\text{pg}}(Q) = \frac{Z^{-1}}{\Omega - \Omega_q + \mu_{\text{pair}} + i\Gamma_Q}, \tag{22}$$

where we associate

$$\Omega_{\mathbf{q}} \approx \frac{q^2}{2M^*}. \tag{23}$$

This establishes a quadratic pair dispersion and defines the effective pair mass, M^*. This can be calculated via a small q expansion of $\chi(Q)$,

$$Z = \left.\frac{\partial\chi}{\partial\Omega}\right|_{\Omega=0,\mathbf{q}=0}, \quad \frac{1}{2M^*} = -\left.\frac{1}{6Z}\frac{\partial^2\chi}{\partial q^2}\right|_{\Omega=0,\mathbf{q}=0}. \tag{24}$$

Finally, one can rewrite Eq. (20) as

$$\Delta_{\text{pg}}^2(T) = Z^{-1}\sum_{\mathbf{q}} b(\Omega_q), \tag{25}$$

where $b(x)$ is the Bose distribution function.

The superfluid transition temperature T_c is determined as the lowest temperature(s) in the normal state at which noncondensed pairs exhaust the total weight of Δ^2 so that $\Delta_{\text{pg}}^2 = \Delta^2$. Solving for the "transition temperature" in the absence of pseudogap effects[21,49,77] leads to the quantity T_c^{MF}. More precisely, T_c^{MF} should be thought of as the temperature at which the excitation gap $\Delta(T)$ vanishes. This provides a reasonable estimate for the pairing onset temperature T^*. It is to be distinguished from T_c, below which a stable superfluid phase exists. We note that T^* represents a smooth crossover rather than a thermodynamic phase transition.

It should be stressed that the dispersion relation for the noncondensed pairs is quadratic. While *one will always find a linear dispersion in the collective mode spectrum*,[18] within the present class of BCS-BEC crossover theories, the restriction to a T-matrix scheme means that there is no feedback from the collective modes onto the pair excitation spectrum. In effect, the T-matrix approximation does not incorporate pair-pair interactions at a level needed to arrive at this expected linear dispersion in the pair excitation spectrum. Nevertheless, this level of approximation is consistent with the underlying ground state wave function.

III. GENERALIZATION TO INCLUDE POPULATION IMBALANCE

It is relatively straightforward to include a difference in particle number between the two spin species, within the context of the BCS-Leggett wave function. This is closely analogous to solving for the spin susceptibility in BCS theory. The excitation energies are given by $E_{k\uparrow}=-h+E_k$ and $E_{k\downarrow}=h+E_k$, where $\xi_k=\epsilon_k-\mu$ and $E_{\mathbf{k}}=\sqrt{\xi_{\mathbf{k}}^2+\Delta^2}$. Here $\mu=(\mu_\uparrow+\mu_\downarrow)/2$ and $h=(\mu_\uparrow-\mu_\downarrow)/2$. We assume spin up fermions are the majority so that $n_\uparrow > n_\downarrow$ and $h>0$. It is important to note that depending on h, μ, and Δ, the quantity $E_{k\uparrow}$ may on occasion assume negative values for a bounded range of k-states. At $T=0$ this implies that there are regimes in k-space in which no minority component is present. This leads to what is often referred to as a "gapless" phase. It was first studied by Sarma[78,79] at $T=0$ in the BCS regime.

It is natural to extend this ground state Sarma or "breached pair" phase to include BCS-BEC crossover effects.[79–83] The effects of finite temperatures were also studied using the current GG_0, T-matrix scheme,[49,76,84,85] using the Nozières Schmitt-Rink formalism[86] as well as using an alternative many body approach.[77,83] It should be noted, however, that the Sarma phase is generally not stable at $T=0$ except on the BEC side of resonance. Studies of the Sarma phase closer to unitarity and at low temperature reveal negative superfluid density[80] as well as other indications for instability.[85] More generally, closer to unitarity, the Sarma phase stabilizes only at intermediate temperatures,[84] while the ground state appears to exhibit phase separation.

The notion of phase separation between paired and unpaired states, separated by an interface, was first introduced[87] in the BCS limit, and it was more extensively discussed at $T=0$ in the crossover regime in Ref. 81 for the homogeneous case. The presence of phase separation in a trap at zero[82,83] and at finite temperature[77,88] has received considerable recent attention. In a harmonic trap, phase separation leads to a nearly unpolarized gas at the center surrounded by a polarized, but essentially uncorrelated normal Fermi gas. Here one sees that the excitation gap Δ decreases abruptly to zero. By contrast, at higher temperatures, where the Sarma phase is stabilized, Δ decreases to zero continuously and there is a highly correlated mixed normal region separating a superfluid core and normal (uncorrelated) gas.

We now extend the present GG_0 formalism to include polarization effects.[23] Including explicit spin indices, the pair susceptibility is given by

$$\chi(Q)=\frac{1}{2}[\chi_{\uparrow\downarrow}(Q)+\chi_{\downarrow\uparrow}(Q)]=\sum_{\mathbf{k}}\left[\frac{1-\bar{f}(E_{\mathbf{k}})-\bar{f}(\xi_{\mathbf{q-k}})}{E_{\mathbf{k}}+\xi_{\mathbf{q-k}}-i\Omega_l}u_{\mathbf{k}}^2 - \frac{\bar{f}(E_{\mathbf{k}})-\bar{f}(\xi_{\mathbf{q-k}})}{i\Omega_l+E_{\mathbf{k}}-\xi_{\mathbf{q-k}}}v_{\mathbf{k}}^2\right], \tag{26}$$

where the coherence factors $u_{\mathbf{k}}^2, v_{\mathbf{k}}^2=(1\pm\xi_{\mathbf{k}}/E_{\mathbf{k}})/2$ are formally the same as for an equal spin mixture. For notational convenience we define

$$\bar{f}(x)\equiv[f(x+h)+f(x-h)]/2. \tag{27}$$

Following the same analysis as for the unpolarized case, and using the above form for the pair susceptibility, the gap equation can be rewritten as

$$-\frac{m}{4\pi a}=\sum_{\mathbf{k}}\left[\frac{1-2\bar{f}(E_{\mathbf{k}})}{2E_{\mathbf{k}}}-\frac{1}{2\epsilon_{\mathbf{k}}}\right]. \tag{28}$$

The mean field number equations can be readily deduced

$$n_\sigma=\sum_{\mathbf{k}}[f(E_{\mathbf{k}\sigma})u_{\mathbf{k}}^2+f(-E_{\mathbf{k}\bar{\sigma}})v_{\mathbf{k}}^2], \tag{29}$$

where the spin index $\sigma=\uparrow,\downarrow$, and $\bar{\sigma}=-\sigma$ is antiparallel to σ. The pseudogap equation is then

$$\Delta_{pg}^2(T)=Z^{-1}\sum_{\mathbf{q}}b(\Omega_{\mathbf{q}}). \tag{30}$$

Analytical expressions for Z and Ω_q can be obtained via expansion of $\chi(Q)$ at small Q (see, e.g., Ref. 23). This theory can readily be extended to include a (harmonic) trap as will be discussed in more detail in Sec. VI. In case of a phase separation, equilibrium requires T, μ, and the pressure, p to be continuous across the interface or domain wall. Finally, it is useful to define polarization δ in terms of

$$N_\sigma(r)=\int d^3r\, n_\sigma(r), \quad N=N_\uparrow+N_\downarrow, \tag{31}$$

$$\delta=(N_\uparrow-N_\downarrow)/N. \tag{32}$$

In this paper we do not discuss alternative phases such as the Larkin-Ovchinnikov-Fulde-Ferrell states[51] in which the condensate is associated with one or more nonzero momenta $\mathbf{q}$. The competition between various polarized phases is associated[23] with the detailed structure of $\chi(Q)$. Indeed, there are strong similarities between these competing phases in polarized gases and Hartree-Fock theories which are used to establish whether ferro- or antiferromagnetic order will arise in a many body system. The latter is associated with zero or finite wave-vector, respectively, and depends on the nature of the particle-hole spin susceptibility, $\bar{\chi}^{\text{part-hole}}(Q)$. This, in turn, is given by $\bar{\chi}^{\text{part-hole}}(Q)\propto\bar{U}^{-1}+\bar{\chi}_o(Q)$, where $\bar{\chi}_o$ is the usual Lindhard function and $\bar{U}$ is the on-site repulsion. Here, by analogy the "ferromagnetic" case would correspond to the Sarma phase and the "antiferromagnetic" situation to a LOFF like phase. Note, however, that the relevant $\chi(Q)$ necessarily involves the self-consistently determined fermionic gap parameter $\Delta(T)$ and chemical potential μ, whereas for the magnetic analogue the bare particle-hole susceptibility appears.

IV. NORMAL-PHASE SELF-CONSISTENT EQUATIONS

We next summarize the self-consistent equations associated with the normal phase. We do not solve these at an exact level. This would require a numerical solution of the T matrix theory above T_c, which has been shown elsewhere[89] to be very complicated. Instead we extend our more precise $T \le T_c$ equations in the simplest fashion above T_c, by continuing to parametrize the pseudogap contribution to the self energy in terms of an effective excitation gap Δ, using Eq. (18), and thereby, ignoring the finite lifetime associated with the normal state (preformed) pairs. We will, however make some accommodation of this lifetime in the following section. The self-consistent gap equation is obtained from Eqs. (21) and (14) as

$$t_{\mathrm{pg}}^{-1}(0) = Z\mu_{\mathrm{pair}} = U^{-1} + \chi(0), \tag{33}$$

which yields

$$U^{-1} + \sum_{\mathbf{k}} \frac{1 - 2f(E_{\mathbf{k}})}{2E_{\mathbf{k}}} = Z\mu_{\mathrm{pair}}. \tag{34}$$

Similarly, above T_c, the pseudogap contribution to $\Delta^2(T) = \Delta_{\mathrm{sc}}^2(T) + \Delta_{\mathrm{pg}}^2(T)$ is given by

$$\Delta_{\mathrm{pg}}^2 = \frac{1}{Z}\sum_{\mathbf{q}} b(\Omega_{\mathbf{q}} - \mu_{\mathrm{pair}}). \tag{35}$$

The density of particles can be written as

$$n = 2\sum_{\mathbf{k}} [u_{\mathbf{k}}^2 f(E_{\mathbf{k}}) + v_{\mathbf{k}}^2 f(-E_{\mathbf{k}})]. \tag{36}$$

It should be understood that the parameters appearing in the expansion of the T-matrix such as Z and Ω_q [see Eq. (22)] are all self-consistently determined as in the superfluid state.

In summary, when the temperature is above T_c, the order parameter is zero, and $\Delta = \Delta_{\mathrm{pg}}$. Since there is no condensate, μ_{pair} is nonzero, thus the gap equation is modified as $t_{\mathrm{pg}}^{-1} = U^{-1} + \chi(0) = Z\mu_{\mathrm{pair}}$. The number equation remains unchanged. From the above three equations, one can determine μ, Δ, and μ_{pair}.

V. APPROXIMATE TREATMENT OF PAIR LIFETIME EFFECTS

In the previous section, we discussed the extension of our more precise $T \le T_c$ equations above T_c, by continuing to parametrize the pseudogap contribution to the self energy in terms of an effective excitation gap Δ, using Eq. (18), and thereby, ignoring the finite lifetime associated with the normal state (preformed) pairs. We will now make some accommodation of this lifetime by including "cutoff" effects associated with an upper limit of the momentum to be inserted into Eq. (35) or Eq. (30).

Below T_c, we can to a good approximation neglect the cutoff for the boson momentum q in evaluating the noncondensed pair contributions to the pseudogap. This is justified by virtue of the divergence of $t_{\mathrm{pg}}(Q)$ at $Q=0$ and low T so that the dominant contributions come from small q pairs. However, above T_c, pairs develop a finite chemical potential so that $t_{\mathrm{pg}}(Q)$ no longer diverges and high momentum pairs would make substantial contributions to the integral in evaluating Δ_{pg} via Eq. (35).

In order to make a more accurate evaluation, we take into account some aspects of the finite lifetime effects of the pairs. From Eq. (7), one can read off the imaginary part as

$$\begin{aligned} \mathrm{Im}\,\chi(\Omega + i0^+, \mathbf{q}) = Z\Gamma_{\Omega,\mathbf{q}} = \frac{\pi}{2}\sum_{\mathbf{k}} [1 - f(E_{\mathbf{k}}) - f(\xi_{\mathbf{k-q}})]u_{\mathbf{k}}^2 \delta(E_{\mathbf{k}} \\ + \xi_{\mathbf{k-q}} - \Omega) + [f(E_{\mathbf{k}}) - f(\xi_{\mathbf{k-q}})]v_{\mathbf{k}}^2 \delta(E_{\mathbf{k}} \\ - \xi_{\mathbf{k-q}} + \Omega), \end{aligned} \tag{37}$$

where $\Gamma_{\Omega,\mathbf{q}}$ is the imaginary part of the pair dispersion. It is clear that $\Gamma_{\Omega,\mathbf{q}}$ is nonzero when $-\min(E_{\mathbf{k}} - \xi_{\mathbf{k-q}}) < \Omega < \min(E_{\mathbf{k}} + \xi_{\mathbf{k-q}})$ for any given $(\Omega, \mathbf{q})$. For on-shell pairs, we set $\Omega = \Omega_{\mathbf{q}} - \mu_{\mathrm{pair}}$ in evaluating $\Gamma_{\Omega,\mathbf{q}}$. Nevertheless, $\Gamma_{\Omega,\mathbf{q}}$ remains small for a large range of momentum $\mathbf{q}$. Here we focus on positive pair dispersion so that the second term in Eq. (37) vanishes. Apart from energy conservation imposed by the delta function, the factor $1 - f(E_{\mathbf{k}}) - f(\xi_{\mathbf{k-q}})$ guarantees that the contribution of the first term in Eq. (37) is very small when $\xi_{\mathbf{k-q}} < 0$ except at high T. As a very good estimate, we impose a cutoff for q such that when $q = q_{\mathrm{cut}}$we have $\Omega_q - \mu_{\mathrm{pair}} = E_{\mathbf{k}} + \xi_{\mathbf{k}}$, where k minimizes $|\xi_{\mathbf{k}}|$. To keep our calculations self-consistent, we also impose this momentum cutoff below T_c.

At high enough T in the BCS and unitary regimes, we sometimes find that there is no solution for q_{cut} when Δ becomes small and $-\mu_{\mathrm{pair}}$ becomes large. We then extrapolate q_{cut} smoothly to zero at higher T via $q_{\mathrm{cut}} \propto \sqrt{\Delta}$. This avoids the unphysical abrupt shut down of the pseudogap at high T. In the BEC regime, however, one finds that $q_{\mathrm{cut}} = +\infty$ and the pairs are bound and long lived, as expected physically.

VI. DENSITY PROFILES

We now turn to include trap effects, with spherical trap potential $V_{\mathrm{ext}}(r) = \frac{1}{2}m\omega^2 r^2$. We emphasize that we will work exclusively within the local density approximation here, and that there are concerns about this approximation in the presence of population imbalance and in highly anisotropic traps.[90] BdG approaches[21,22] as well reveal that extreme anisotropy (which we will not address here) cannot be addressed with the LDA.

Within a trap, we impose the force balance equation, $-\nabla p = n\nabla V_{\mathrm{ext}}$, where p is the pressure and V_{ext} is the trap potential. In the trap, the temperature is constant, so we have the relation $\nabla p = n\nabla\mu$. Thus we obtain $\nabla\mu = -\nabla V_{\mathrm{ext}}(r)$, or

$$\mu(r) = \mu_0 - V_{\mathrm{ext}}(r), \tag{38}$$

where $\mu_0 \equiv \mu(0)$ and $V_{\mathrm{ext}}(0) = 0$. This shows that the force balance condition naturally leads to the usual local density approximation (LDA) in which the fermionic chemical potential μ can be viewed as varying locally, but self-consistently throughout the trap.

We can readily extend our self-consistent equations from the previous sections to incorporate a trap, treated at the level of LDA. T_c is defined as the highest temperature at which the self-consistent equations are satisfied precisely at the trap center. At a temperature T lower than T_c the superfluid region

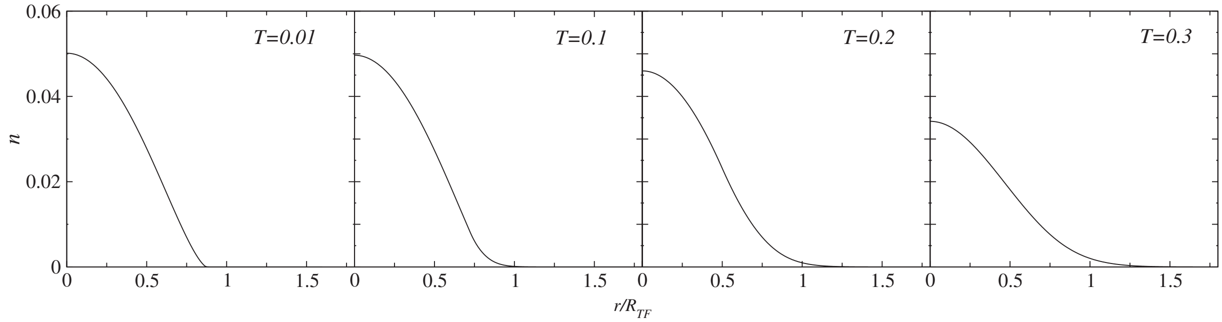

FIG. 2. 3D density profiles $n(r)$ of a Fermi gas in a harmonic trap at unitarity at T/T_F=0.01, 0.1, 0.2, and 0.3. The density distributions are smooth and monotonic, and become broader with T increasing. There is no bimodal feature in the density profiles, in agreement with experimental observations. Here $T_F=E_F/k_B$ is the global Fermi temperature and R_{TF} is the Thomas-Fermi radius. The density $n(r)$ is in units of k_F^{-3}. At unitarity, $T_c=0.28T_F$.

extends to a finite radius R_{sc}. The particles outside this radius are in a normal state, with or without a pseudogap. The important chemical potential $\mu_{\mathrm{pair}}(r)$ is identically zero in the superfluid region $r<R_{\mathrm{sc}}$, and must be solved for self-consistently at larger radii. Our calculations proceed by numerically solving the self-consistent equations. In the figures below, we express length in units of the Thomas-Fermi radius $R_{\mathrm{TF}}=\sqrt{2E_F/(m\omega^2)}=2(3N)^{1/3}/k_F$; the density $n(r)$ and total particle number $N=\int d^3\mathbf{r}\, n(r)$ are normalized by k_F^3 and $(k_F R_{\mathrm{TF}})^3$, respectively.

We determine T_c as follows: (i) An estimated initial value for chemical potential is assigned to the center of the trap $\mu(0)$, which determines the local $\mu(r)=\mu(0)-V_{\mathrm{ext}}(r)$. (ii) We solve the gap equation (1) and pseudogap equation (35) at the center (setting $\Delta_{\mathrm{pg}}=\Delta$) to find T_c and $\Delta(0,T_c)$. (iii) We next determine the radius $R_{\max}$ where Δ drops to zero. (iv) Next we solve the gap equation (34) and pseudogap equation (35) for $\Delta(r,T_c)$ for $r\leq R_{\max}$. Then $n(r)$ is determined using Eq. (36). (v) We integrate $n(r)$ over all space and enforce the total number constraint $N=\int d^3r\, n(r)$. We use nonlinear equation solvers which iteratively find the solution for the global $\mu(0)$ and the local gap parameters. Below T_c, an extra step is involved to determine the condensate edge, R_{sc}, where Δ_{sc} drops to zero. Within the superfluid core, Eqs. (1) and (35) are solved locally for Δ and Δ_{sc}, with $\mu_{\mathrm{pair}}(r)=0$.

A. Numerical results for unpolarized case

In this section we address the particle density profiles at all T in the near-BEC, the near-BCS, and the unitary regimes. For the latter, this work helps to establish why the measured density profiles for an unpolarized gas appear to be so featureless.[91,92] It should be stressed that this is stark contrast with what one sees for the polarized case, as will be discussed below. Some time ago it was found[91] that at unitarity the profiles were reasonably well described by a Thomas-Fermi (TF) fit at zero T, and in recent work[93] this procedure has been extended to finite temperatures, suggesting that it might be quite general. Our calculations indicate this TF fit is reasonably good below T_c, and becomes substantially better above T_c. The width of the profiles has been used to extract an effective temperature scale.[93] If we follow the same procedure[48] on our theoretical profiles we find that the temperature scale coincides with the physical T quite precisely above T_c. Below T_c, because the condensate edge moves inwards as temperature increases, this tends to compensate for thermal broadening effects. In this way, in the superfluid phase the effective temperature needs to be recalibrated[48] to arrive at the physical temperature scale.

Within the (same) LDA approximation, our work differs from previous theoretical studies[15,94,95] by including the important effects of noncondensed pairs[3,42] which are associated with pseudogap effects. These "bosons" are principally in the condensate region of the trap, whereas fermionic excitations tend to appear at the edge where the gap is small. In contrast to the work of Refs. 68 and 43, our density profiles are monotonic in temperature and show none of the sharp features in the BEC which were predicted[43] from a generalization of the Nozières–Schmitt-Rink approach (in the absence of population imbalance and phase separation). Our calculations show that pseudogap effects are responsible, not only for the relatively featureless density profiles we find in the unitary regime, but also for the behavior of the associated temperature evolution. It should be noted that except in certain extreme cases (e.g., high anisotropy or very low particle number), LDA is an appropriate approximation, as has been widely used.

Figure 2 shows the behavior of the three-dimensional (3D) density profiles of a Fermi gas at unitarity as temperature progressively increases (from left to right). One can see that the profiles become progressively broader with increasing T. Because there is no bimodality or other reflections of the condensate edge, one can thereby understand why the Thomas-Fermi fits are not inappropriate. A more quantitative comparison of this unitary case with experiment is in Ref. 96.

In Fig. 3 we present a comparison of the density profiles in a unitary system with the near BEC and near BCS cases. On the BEC side of resonance $(1/k_Fa=1)$ the profile is significantly narrower than that on the BCS side. The unitary case is somewhere in between. The quantity β which is used in the literature to parametrize this width is approximately -0.41 as compared with experiment[92] where $\beta\approx-0.55$. Conventionally, β is defined as the ratio of the attractive interaction energy to the kinetic energy and is given by $\mu=(1$

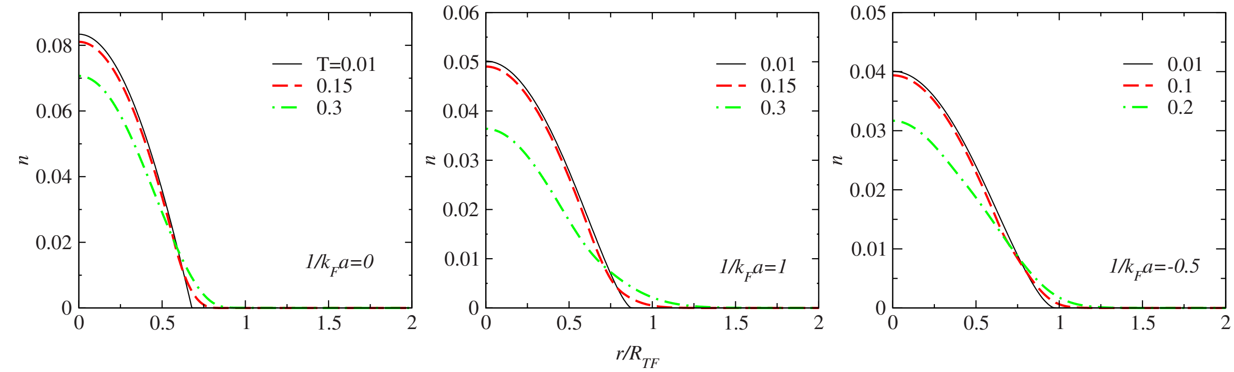

FIG. 3. (Color online) Comparison of 3D density profiles $n(r)$ at different temperatures between the unitary (left), near BEC ($1/k_F a=1$, middle), and near BCS ($1/k_F a=-0.5$, right panel) regimes. They broaden with increasing T but shrink with increasing pairing strength. From left to right, T_c=0.28, 0.34, and 0.20T_F, respectively.

$+\beta)E_F$ and $\mu_0=\sqrt{1+\beta}E_F$ for homogeneous and trapped unitary gases, respectively. The discrepancy between theory and experiment is associated with the absence of Hartree self-energy corrections in the BCS-Leggett mean field state. Thus, for more quantitative comparison with unitary experiments[48] we match the measured β factor by going slightly on the BEC side of resonance.

B. Phase diagrams in the polarized case

The phase diagrams for polarized gases are a very useful way to consolidate information about the competing phases and their temperature dependencies. They can also be used to read off the transition temperatures T_c both at zero and finite polarization, which are relevant to all figures in this and subsequent sections. Figure 4 presents a plot of the phase diagram of the unitary gas in the homogeneous case. These results are consistent with previous LDA studies[83,97] which have addressed the strict ground state. Phase separation (labeled PS) occupies the lower T portion of the phase diagram.[98] At intermediate T, and sufficiently small polarization, there is a Sarma phase (yellow), where there is homogeneous superfluidity but with pairs having net zero momentum. We indicate the correlated normal or pseudogap regime by "pseudogap" (cyan) and the uncorrelated or unpaired normal phase by "*N*." The line for T^* which separates N from pseudogap phases should be viewed as a lower bound, since at the very edge of this interface, for numerical reasons, we cut Δ off sharply to zero.

Figure 5 presents a plot of the unitary gas phase diagram in the presence of a trap. It can be seen that in a trap, the Sarma phase occupies a much more substantial portion of the phase diagram. This is because the trap center can be maintained at very small population imbalance, whereas the normal fluid at the edge is able to carry most of the excess majority population. Our results are very similar to those we published earlier[88] except that here we have incorporated cutoff effects as described above, so that the indicated T^*

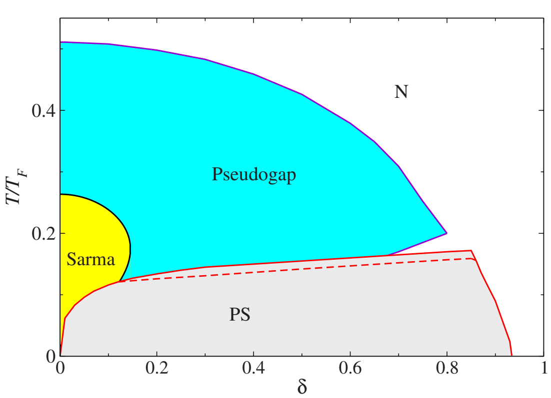

FIG. 4. (Color online) Phase diagram in the T-δ plane of a homogeneous population imbalanced Fermi gas at unitary. The important point is to distinguish between two types of normal phases. "*N*" corresponds to effectively noninteracting Fermi gas whereas "pseudogap" corresponds to pseudogapped normal phase. The low T phase separated state we find is always associated with the Fermi gas, not a paired normal state. While one can read off the pair formation crossover temperature T^* from this plot, it should be viewed as a lower bound, due to our cutoff procedure described in Sec. V, which may or may not also account for the small missing wedge of the pseudogap regime.

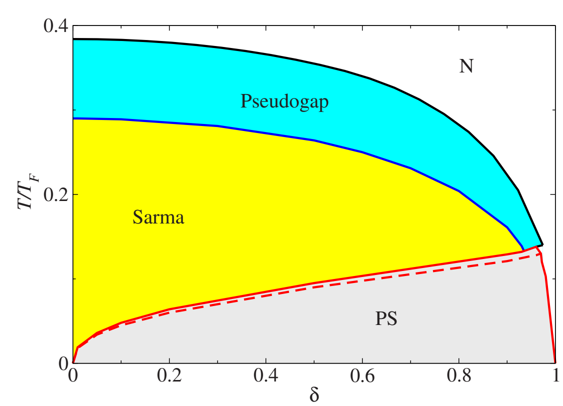

FIG. 5. (Color online) Phase diagram in the T-δ plane of a trapped population imbalanced Fermi gas at unitary. The labels have the same meaning as Fig. 4. T=0 is always phase separated state. These results are only very slightly modified relative to those in Ref. 88 as a result of our cutoff procedure described in Sec. V.

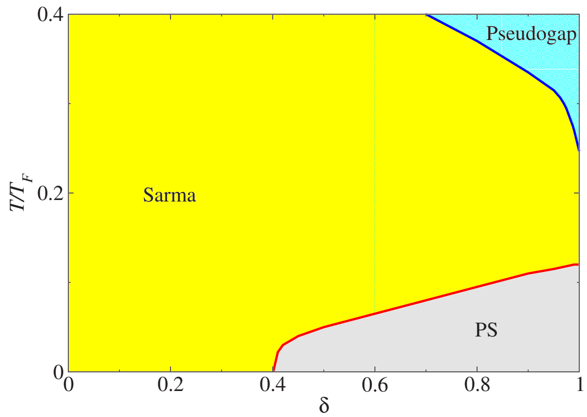

FIG. 6. (Color online) Phase diagram in the T-δ plane of a trapped population imbalanced Fermi gas at $1/k_Fa=1.5$ in the BEC regime. Here PS denotes phase separation, which exists only at low T and high polarization.

should be viewed as a lower bound. Here, too, phase separation occupies the lowest portion of the phase diagram. In this regime the gap Δ jumps abruptly to zero at a fixed trap radius. The Sarma state is found at intermediate T and associated with more continuous behavior in Δ as a function of trap radius. It can be seen that, away from $p=0$, a minimum temperature is required to arrive at the Sarma phase. The latter evolves into a pseudogap phase at higher temperatures when the superfluid core vanishes. An unpaired, normal phase is always found at the highest T.

Finally, Fig. 6 shows the phase diagram at $1/k_Fa=1.5$ on the BEC side of resonance in the presence of a trap. This should be compared with the counterpart phase diagram for a unitarity gases in Fig. 5 as well as with that in the near-BCS which was presented in Ref. 88. The principal difference between unitarity and this case is that for the former the phase separation (PS) region is present at low T over the entire range of polarizations, whereas in the BEC regime, it has been pushed toward the high polarization region of the phase diagram.

C. Numerical results for density profiles in polarized case

In this section we show how the general shape of the density profiles at unitarity changes as one varies the polarization. Unlike the unpolarized case, we can identify features in the polarized gas profiles which indicate whether or not the gas is superfluid; these features are rather similar to what is observed experimentally.[53,77,99,100] We also trace the evolution of the profiles from phase separation at low temperature to the Sarma phase.

Figure 7 shows the temperature dependence of the unitary profiles for majority and minority spin components at $p=0.5$ for a range of temperatures, increasing from left to right. The lowest temperature ($T/T_F=0.01$) corresponds to a situation when phase separation is present, while the three higher temperature correspond to the Sarma phase. The condensate edge is clearly apparent in the phase separation scenario, with a jump in the order parameter (and a discontinuity in the density) at the edge. For the Sarma phase cases, bimodality is clearly visible in the minority profile, and a kinklike feature is present in the majority profile well below T_c. At high T, both majority and minority profiles become closer to a Thomas-Fermi distribution, as polarization has penetrated into the superfluid core.

The two vertical dashed lines for the three Sarma cases in the figure delimit the paired normal region. They correspond to the condensate edge, where Δ_{sc} drops to 0, and the gap edge where the total excitation gap $\Delta=\Delta_{pg}$ smoothly disappears. Between the two dashed lines the system is in a paired or highly correlated mixed normal state.[99,100] The width of this mixed normal region grows with increasing temperature, and the condensate edge disappears above T_c. Outside the gap edge, the gas is free; there is a small range of r where both spin components are present and a wider range where only the majority appears. In the phase separation regime, such a mixed normal region is essentially absent,[53] and the condensate edge is indicated by a single dashed vertical line. For low T, we note that the condensate is essentially unpolarized. Finally, it should be stressed that experiments observe a complex phase diagram[77] in which both phase sepa-

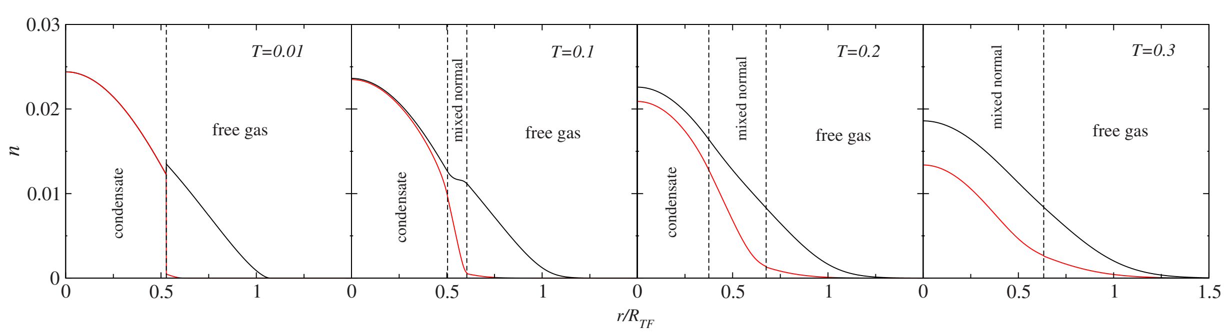

FIG. 7. (Color online) Evolution of the 3D density profiles $n(r)$ with temperature T at unitarity and polarization $\delta=0.5$. The upper (black) and lower (red) curves are for the majority and minority species, respectively. From left to right, $T/T_F=0.01$, 0.1, 0.2, and 0.3. Phase separation occurs for $T/T_F=0.01$, where the profile shows abrupt changes at the phase boundary, whereas the Sarma phase prevails in the other cases so that the profiles are smooth. Bimodality is clearly visible in the Sarma cases. Within the vertical dashed lines there exists a paired normal region. Here "free Fermi gas" is distinguished from the "mixed normal" regime in that the former, unlike the latter, contains no pairing correlations or pseudogap. Note that in the left panel ($T=0.01T_F$) the densities *in the condensate core* for both spins are the same so that the red curve overlays on top of the black one in this region. The density discontinuity across the phase boundary for $T=0.01T_F$ is a necessary consequence of phase separation. Here $T_c=0.26T_F$.

ration (at the lowest T) and a Sarma or Sarma-like phase (at higher T) is present.

In summary, in the phase separation regime, there are sharp discontinuities in the profile associated with the condensate edge, the other side of which is a free Fermi gas. By this "free Fermi gas" we mean an uncorrelated or unpaired phase in which one or both spin components is present. In the Sarma phase, which is stabilized at higher T, there may also be indications of the condensate edge. Beyond the superfluid core, there is a highly correlated mixed normal region which carries a significant fraction of the polarization and is associated with the pseudogap phase. Finally, in the outer regime of the profile there is a free Fermi gas, which may consist of majority only or of both spin states. These three regions in the Sarma phase seem to be in accord with experiment.[99,100] An important additional finding is that except at high temperatures the superfluid core seems to be robustly maintained at nearly zero polarization, as observed experimentally.[53,77,99,100]

VII. THERMODYNAMICS

In this section we introduce[101] an approximate form for the thermodynamical potential (density), Ω. We can, to a high level of accuracy, write this down analytically. It is important to assess this approximate form by studying various thermodynamical identities. We will do so here by checking Maxwell's relations as well as establishing the relationship $p=\frac{2}{3}E$ between energy density E and pressure p, which is expected[15,16] to apply at strict unitarity. In the superfluid phase, we find there is essentially no deviation from the precise thermodynamical relations. Above T_c, we find deviations of from one to a few percent.

We begin with the unpolarized case. The quantity Ω is associated with a contribution from gapped fermionic excitations Ω_f as well as from noncondensed pairs, called Ω_b. These two contributions are fully interdependent. The gap in the fermionic excitation spectrum is present only because there are pairs and conversely. In this section, we will use the notation $\Omega_{\mathbf{q}}=q^2/2M^*-\mu_{\text{pair}}$. We have

$$\Omega=\Omega_f+\Omega_b,$$

$$\Omega_f=\Delta^2\chi_0+\sum_{\mathbf{k}}\left[(\xi_{\mathbf{k}}-E_{\mathbf{k}})-2T\ln(1+e^{-E_{\mathbf{k}}/T})\right],$$

$$\Omega_b=\sum_{\mathbf{q}}T\ln(1-e^{-\Omega_{\mathbf{q}}/T}), \tag{39}$$

where $\chi_0\equiv -U^{-1}-Z\mu_{\text{pair}}$. The pressure is simply

$$p=-\Omega. \tag{40}$$

Here $\mu_{\text{pair}}=0$ at $T\leq T_c$, while above T_c the superconducting order parameter $\Delta_{\text{sc}}=0$. Providing that we ignore the very weak dependence of the parameter Z and the pair mass M^* on Δ, μ, and h, we are able to derive our self-consistent gap, pseudogap, and number equations variationally. These self-consistent (local) equations are given by

$$\frac{\partial\Omega}{\partial\Delta}=0, \tag{41}$$

which represents the gap equation (34). Similarly, we have

$$\frac{\partial\Omega}{\partial\mu_{\text{pair}}}=0, \tag{42}$$

which leads to the equation for the pseudogap given by Eq. (35). Finally, the number equation

$$n=-\frac{\partial\Omega}{\partial\mu}, \tag{43}$$

which yields Eq. (36). In a trap, this is subject to the total number constraint $N=\int d^3r\, n(r)$.

From the above thermodynamical potential, we can determine all other thermodynamic quantities. The energy (density) is

$$E=E_f+E_b,$$

$$E_f=-\Delta^2\chi_0+\sum_{\mathbf{k}}\left[(\xi_{\mathbf{k}}-E_{\mathbf{k}})-2E_{\mathbf{k}}f(E_{\mathbf{k}})\right]+\mu n,$$

$$E_b=\sum_{\mathbf{q}}(\Omega_{\mathbf{q}}+\mu_{\text{pair}})b(\Omega_{\mathbf{q}}), \tag{44}$$

and the entropy (density) is

$$S=S_f+S_b,$$

$$S_f=2\sum_{\mathbf{k}}\left[\frac{E_{\mathbf{k}}}{T}f(E_{\mathbf{k}})-\ln(1+e^{-E_{\mathbf{k}}/T})\right],$$

$$S_b=\sum_{\mathbf{q}}\left[\frac{\Omega_{\mathbf{q}}}{T}b(\Omega_{\mathbf{q}})+\ln(1-e^{-\Omega_{\mathbf{q}}/T})\right]. \tag{45}$$

It is easy to verify the relation

$$\Omega_f=E_f-TS_f-\mu n \tag{46}$$

and

$$\Omega_b=E_b-TS_b-\mu_{\text{pair}}n_{\text{pair}}, \tag{47}$$

with $n_{\text{pair}}=Z\Delta_{\text{pg}}^2$.

In the actual calculations of thermodynamic properties we combine Eq. (39) with a microscopic calculation of the noncondensed pair propagator, thereby determining Z, and Ω_q from the expansion of the inverse T-matrix. We test the validity, then, of our expression for the thermodynamic potential Ω by examining Maxwell identities. Indeed the deviation is generally at most at the few percent level, as will be illustrated below.

Finally, we end our analytical discussion with expressions for a polarized gas. Here the thermodynamical potential is given by

$$\Omega=\Omega_f+\Omega_b,$$

$$\Omega_f=\Delta^2\chi_0+\sum_{\mathbf{k}}(\xi_{\mathbf{k}}-E_{\mathbf{k}})-\sum_{k,\sigma}T\ln(1+e^{-E_{k,\sigma}/T}),$$

$$\Omega_b = \sum_{\mathbf{q}} T \ln(1 - e^{-\Omega_{\mathbf{q}}/T}). \tag{48}$$

Competing with this phase is the free Fermi gas phase which has thermodynamical potential density

$$\Omega_{\text{free}} = -T \sum_{\mathbf{k},\sigma} \ln(1 + e^{-\xi_{k\sigma}/T}). \tag{49}$$

Here $E_{\mathbf{k}\sigma} = E_{\mathbf{k}} \mp h$ and $\xi_{\mathbf{k}\sigma} = \xi_{\mathbf{k}} \mp h$ for spin $\sigma = \uparrow, \downarrow$, respectively.

It should be noted that in this paper, we are concerned with primarily the *internal* energy (density) and pressure without the contribution from the external trap potential, in order to test the relationship $p/E = 2/3$. The internal energy can be obtained by substituting for the chemical potential the local $\mu(r)$ in the term E_f in Eq. (44). The total energy, which includes the trap potential, may be obtained by further adding $nV_{\text{ext}}(r)$ to E_f in Eq. (44). For a harmonic trap at unitarity, the internal energy and the external trap potential energy are equal.[16]

A. Numerical results for unpolarized case

In this section we discuss numerical results for thermodynamic properties principally for trapped Fermi gases within the unitary, near-BCS and near-BEC regimes. We find that unpaired fermions at the edge of the trap, where Δ is small, provide the dominant contribution to thermodynamical variables such as E and S at all but the lowest T. In addition to the usual gapped fermionic excitations, there are "bosons" which correspond to finite momentum pairs. Above T_c these "bosons" lead to a normal state fermionic excitation gap (or "pseudogap").[3,42,44,102] They are dominant only at very low $T \ll T_c$, leading to $S \propto T^{3/2}$. We emphasize that the normal state of these superfluids is never an ideal Fermi gas, except in the extreme BCS limit, or at sufficiently high T above the pseudogap onset temperature T^*.

In Fig. 8, we plot (a) the energy per particle E/N (dashed lines) multiplied by 2/3 and pressure p/n (solid lines) and (b) the entropy S/Nk_B for a homogeneous system and for a range of values of $1/k_Fa$, from noninteracting ($1/k_Fa = -\infty$) to near BEC ($1/k_Fa = 1/2$). It can be seen that all curves approach the free Fermi gas results at $T > T^*$. It is also clear that, as expected, the energy and entropy are lowered as the system goes deeper into the BEC. The pairing onset temperature T^* stands out in the figure as the most apparent temperature scale. We find virtually no thermodynamic feature at T_c. A small feature should be present in the BEC, becoming larger as the BCS regime is approached. This would appear if we included lifetime effects associated with the noncondensed pairs; in order to make the calculations manageable, we have ignored this complexity which has been addressed elsewhere.[103] It should be stressed that T^* represents a crossover temperature and is not to be associated with singular structure in thermodynamical variables, unlike T_c.

The comparison between the dashed and solid lines in Fig. 8(a) represents an important indicator of the universality expected at strict unitarity, where the energy density and pressure satisfy $p = \frac{2}{3}E$. Indeed the two curves are virtually

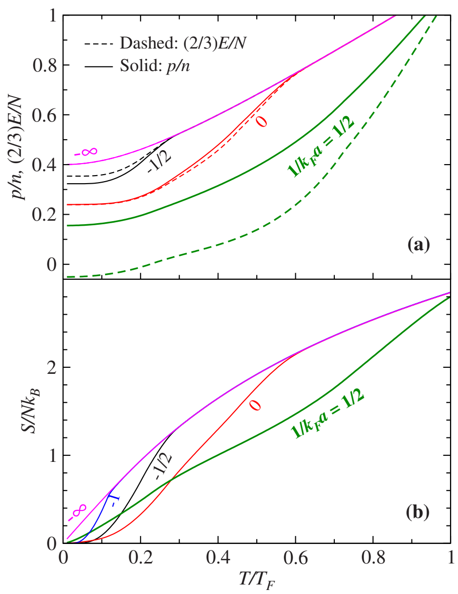

FIG. 8. (Color online) Thermodynamic behavior of a homogeneous Fermi gas at different $1/k_Fa$ as labeled. Shown in (a) the comparison between per-particle energy (multiplied by 2/3, dashed lines) $(2/3)E/N$ and pressure p/n (solid lines) and in (b) the entropy per particle S/Nk_B. Here $N = n$ since we have set volume $V = 1$.

indistinguishable in the superfluid phase at unitarity, and remain very close to each other in the normal phase. This relationship also holds for the noninteracting gas. By contrast, on the BEC side of resonance this relation is seriously violated, as expected.

Figure 9 represents a test of one particular Maxwell relation for the unitary case (upper panel) and for the near-BEC ($1/k_Fa = 1$, lower panel). Here we compare dn/dT (solid lines) with $ds/d\mu$ (dashed lines). The horizontal axis is the trap radius in units of R_{TF}. At the lowest temperature this Maxwell relation is very well satisfied. The feature shown in the plotted derivatives corresponds to the condensate edge. As the temperature is raised the deviation is slight, but perceptible. The small breakdown in the Maxwell relations corresponds to our approximate treatment of the normal phase as discussed in Sec. IV.

In Fig. 10 we plot the trap averaged pressure (per particle) p/N (solid) and $(2/3)E/N$ (dashed lines) in the upper panel as well as entropy S/N in the lower panel, as a function of temperature. For each quantity, the three curves correspond to unitarity and near-BCS ($1/k_Fa = -0.5$) and near-BEC ($1/k_Fa = 1$), respectively, as labeled. As for the homogeneous case in Fig. 8, the closer the system is to BEC the lower the energy and entropy, as expected. Although not shown here, all curves will approach the free Fermi gas curve at sufficiently high T, corresponding to their respective T^*. By comparing the solid and dashed lines in the upper panel, one can see that the relation $p = 2E/3$ is essentially satisfied at unitarity.

Figure 11 plots the spatial distribution of the pressure p (solid) and the energy $2E/3$ (dashed lines), as well as the entropy S (inset) for three different temperatures, for the uni-

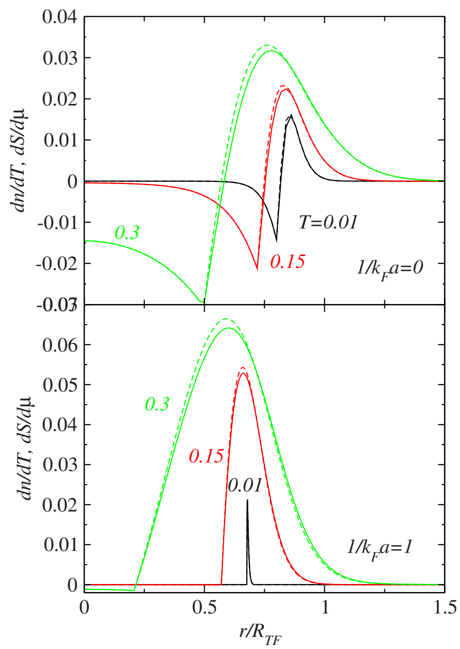

FIG. 9. (Color online) Test of Maxwell relations. The solid and dashed curves are dn/dT and $ds/d\mu$, respectively, as function of trap radius, at different temperatures for $1/k_Fa=0$ (upper) and $1/k_Fa=1$ (lower panel). As labeled, the black, red, and green colors correspond to T/T_F=0.01, 0.15, and 0.3, respectively. The difference between the solid and dashed curves, while largest in the normal regime, is almost negligible.

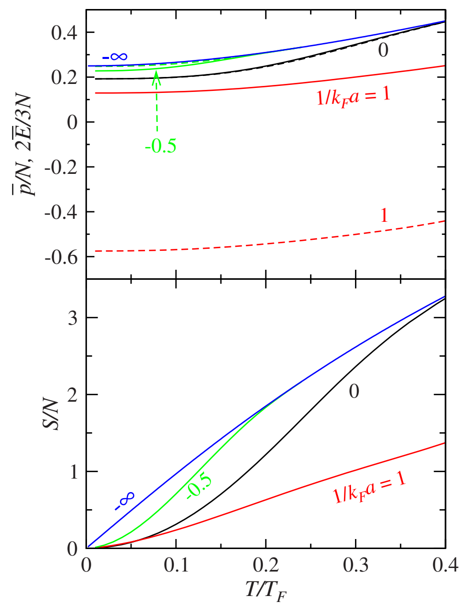

FIG. 10. (Color online) Trap averaged (per-particle) pressure $\bar{p}/N$ (solid), and internal energy $\bar{E}/N$ in the upper panel and entropy S/N in the lower panel as a function of T for $1/k_Fa$=−0.5, 0, and 1, as labeled. The relation $p=2E/3$ is satisfied for and only for the unitary case. The agreement is nearly perfect at $T<T_c$. In the pseudogap phase, the discrepancy remains very small (<5%). Here the contribution from the *external* trap potential is not included in the $\bar{p}$ or $\bar{E}$. T_c/T_F=0.19, 0.28, and 0.33, respectively, for the three regimes.

tary (upper panel) and the near BEC ($1/k_Fa=1/2$, lower panel) cases, respectively. The relation $p/E=2/3$ holds very well at unitarity for all temperatures shown, but, as expected, it is clearly violated in the near BEC case. For $1/k_Fa=1/2$, one sees that the energy becomes negative at intermediate trap radii. This reflects the fact that at these radii, the density is reduced so that the local quantity $1/k_Fa$ is effectively increased and the gas is in the BEC regime. At unitarity the entropy in the inset tends to peak towards the trap edge; this reflects the contribution from free fermions. By contrast these free fermions are relatively absent in the near-BEC case and the entropy is dominated by pair excitations leading to a relatively constant dependence on the trap radius.

B. Numerical results for polarized case

In this section we discuss the behavior of thermodynamical variables for a polarized gas at unitarity. In the upper panel of Fig. 12 we compare the trap averaged pressure per particle, p/N (solid curves) and energy $(2/3)E/N$ (dashed curves) as a function of temperature, for three different polarizations δ=0.1, 0.5, and 0.8. The lower panel shows the corresponding behavior of the entropy S/N. The figure illustrates that the lower the polarization the lower is the energy and entropy. This is because the system can take full advantage of the pairing when the polarization is small. Importantly, the upper panel demonstrates that the relation $p/E=2/3$ also appears to hold for a polarized gas. There are small kinks in the entropy curves at the two higher polarizations which reflect the transition from the phase separated to Sarma state.

The spatial profiles of the three thermodynamical variables are plotted for three different temperatures in Fig. 13 at fixed polarization δ=0.5. The results are not dramatically different from the unpolarized case shown in the upper panel of Fig. 11. One can see that the $p/E=2/3$ relation holds rather well across the trap and that at intermediate temperatures, the entropy tends to peak somewhat inside the trap edge, reflecting the excitations of nearly free fermions in this regime.

VIII. SUPERFLUID DENSITY

An essential component of any theory for BCS-BEC crossover is establishing that the superfluid density is well behaved. The superfluid density $n_s(T)$ is perhaps the best reflection of a proper (or improper) description of the superfluid phase. This meaningful description is not at all straightforward to come by once one includes self-energy corrections to the BCS gap and number equation. These two must be treated on an equal footing in order for the "diamagnetic" and "paramagnetic currents" to precisely cancel at T_c when approached from below.[24,75] (And the T_c that one computes from below has to be the same as that computed from the pairing instability of the normal phase).

This cancellation[75] of diamagnetic and paramagnetic currents is deeply and importantly related to generalized Ward

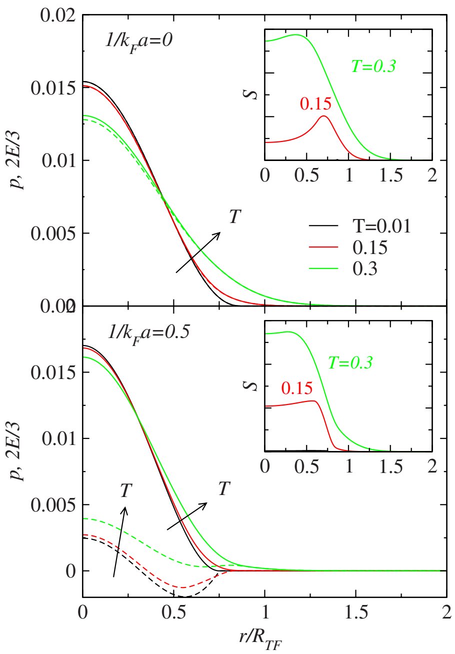

FIG. 11. (Color online) Spatial profile of the pressure $p(r)$ (solid) and internal energy $(2/3)E(r)$ (dashed lines) in the main figures as well as the entropy $S(r)$ in the insets at T/T_F=0.01 (black), 0.15 (red), and 0.3 (green curves), for the unitary (upper panel) and near BEC (lower panel), respectively. The arrows point in the direction of increasing T. At unitarity, the relation $p=2E/3$ is nearly perfect for the low T profiles, while in the pseudogap phase, the deviation is less than 5%. The $1/k_Fa=0.5$ case clearly violates the $p=2E/3$ relation.

identities[18,104] as we will show below. These arise from a connection between the one particle properties (which show up in the diamagnetic current, through the number equation) and the two particle properties (which, for example, reflect the fermionic excitation spectrum $E_{\mathbf{k}}$ and show up in the gap equation). It is important to stress at the outset that because we must distinguish between the gap and the order parameter, *there is no unambiguous way to make use of the Nambu Gor'kov formalism*. One can readily see, however, that the combination GG_0 is, in effect, proportional to that Gor'kov "F" function which involves the full excitation gap Δ, rather than the order parameter.

Whether one considers a charged or an uncharged system, the formal analysis can be made the same.[105,106] For the neutral system one introduces a "fictitious" vector potential and associated charge.[107–109] We consider the magnetic response kernel $K(0)$ in linear response theory. Within the transverse gauge we may write down this response without including the contribution from collective modes. The London penetration depth λ is given by $\lambda_L^{-2}=\mu_0 e^2(n_s/m)$, where μ_0 is the magnetic permittivity. Here we set $\mu_0=e=1$ for convenience. From linear response theory,

$$\lambda_L^{-2} = K_{xx}(0) = \left(\frac{n}{m}\right)_{xx} - P_{xx}(0), \tag{50}$$

where K is defined by

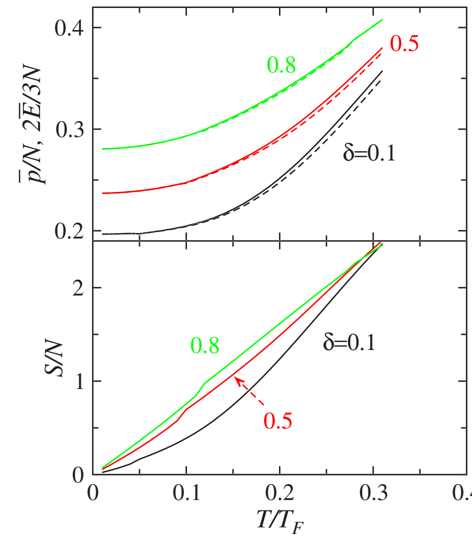

FIG. 12. (Color online) Temperature dependence of the trap averaged pressure $\bar{p}/N$ (solid), internal energy $\bar{E}/N$ (dashed) in the upper panel, and entropy S/N in the lower panel in a trap at unitarity for polarization δ=0.1 (black), 0.5 (red), and 0.8 (green curves), as labeled. The $p=2E/3$ relation is satisfied at unitarity even with population imbalance. The small kink in S/N indicates the change from phase separation to Sarma state. T_c/T_F=0.28, 0.25, and 0.19 for polarization δ=0.1, 0.5, and 0.8, respectively.

$$J_\mu(Q) = P_{\mu\nu}(Q)A_\nu(Q) - \left(\frac{n}{m}\right)_{\mu\nu} A_\nu(Q) = -K_{\mu\nu}(Q)A_\nu(Q), \tag{51}$$

and the current-current correlation function

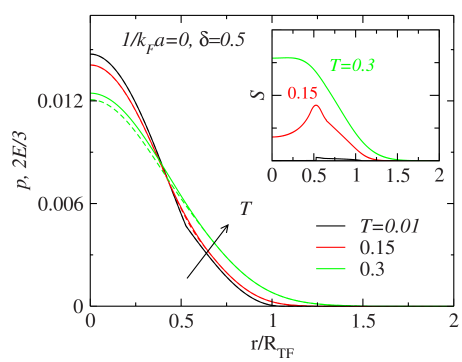

FIG. 13. (Color online) Spatial profiles of pressure (solid) and energy (dashed) in the main figure and entropy in the inset at unitarity and polarization δ=0.5, for T/T_F=0.01 (black), 0.15 (red), and 0.3 (green curves), respectively. The black, red, and green curves correspond to T=0.01, 0.15, and 0.3T_F, respectively. The arrow points along the direction of increasing T. The $p=2E/3$ relation is essentially perfect for low T profiles, and the deviation remains very small ($<5\%$) in the pseudogap phase.

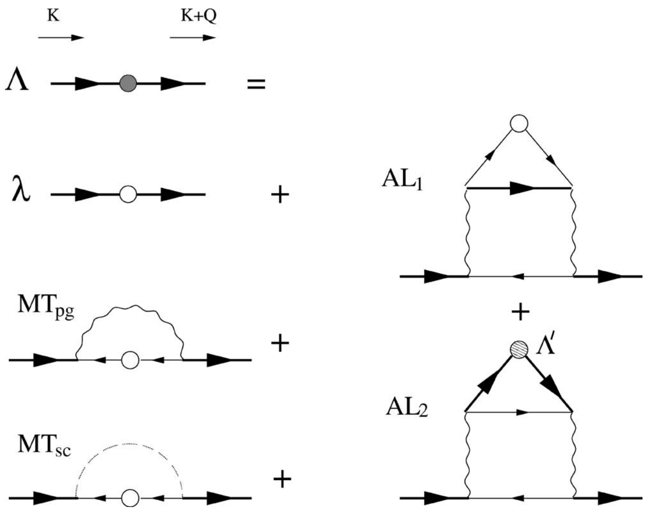

FIG. 14. Diagrams contributing to the full electromagnetic vertex Λ in the transverse gauge. Here the wiggly lines represent the T-matrix t_{pg} and the dashed line represent the singular "condensate propagator" t_{sc}, both shown in Fig. 1. The gauge covariant full vertex Λ' contains the electromagnetic vertex insertion along t_{sc}.

$$
\begin{aligned}
P_{\mu\nu}(Q) &= \int_0^\beta d\tau\, e^{i\Omega_n\tau}\langle j_\mu(\mathbf{q},\tau) j_\nu(-\mathbf{q},0)\rangle \\
&= -2\sum_K \Lambda_\mu(K,K+Q)G(K+Q)\lambda_\nu(K+Q,K)G(K).
\end{aligned}
\tag{52}
$$

Here we use the four-vector notation, $A_\mu=(\phi,\mathbf{A})$, $j_\mu=(\rho,\mathbf{j})$, and the bare vertex $\lambda_\mu=(1,\boldsymbol{\lambda})$. Summation is assumed on repeated indices, with the convention $A_\mu B_\mu=A_0B_0-\mathbf{A}\cdot\mathbf{B}$. Without loss of generality we can ignore collective mode effects and work in a transverse gauge.

For the bare vertex, we have $\lambda_0=1$ and

$$
\boldsymbol{\lambda}(K,K+Q) = \vec{\nabla}_{\mathbf{k}}\epsilon_{\mathbf{k}+\mathbf{q}/2} = \frac{1}{m}\left(\mathbf{k}+\frac{\mathbf{q}}{2}\right),
\tag{53}
$$

The electromagnetic vertex can be written in terms of the corrections coming from the two self-energy components as

$$
\Lambda = \lambda + \delta\Lambda_{pg} + \delta\Lambda_{sc},
\tag{54}
$$

where $\delta\Lambda_{pg}$ is the pseudogap term. This contribution deriving from pair fluctuations contains terms associated with Maki-Thompson (MT) like diagrams as well as Aslamazov-Larkin terms (AL) which appear in the theory of conventional superconducting fluctuations. Here the situation is somewhat more complex because of the appearance of one dressed and one bare Green's function in the pair propagator, which leads to two AL diagrams. As a result the AL term itself depends on a (gauge covariant) vertex function Λ'. We may write

$$
\delta\Lambda_{pg} \equiv \delta\Lambda_{MT} + \delta\Lambda_{AL_1} + \delta\Lambda_{AL_2}(\Lambda').
\tag{55}
$$

The diagrams contributing to the full electromagnetic vertex Λ in the transverse gauge are given in Fig. 14. Here Λ_{MT} is given by the MT$_{pg}$ diagram, and $\delta\Lambda_{sc}$ is given by the MT$_{sc}$ diagram. In contrast to the electromagnetic vertex Λ, the gauge covariant vertex Λ' satisfies a generalized Ward identity to be discussed below.

We now show that there is a precise cancellation between the MT$_{pg}$ and AL$_1$ pseudogap diagrams at $Q=0$. This cancellation follows directly from a generalized Ward identity (GWI)

$$
Q\cdot\lambda(K,K+Q) = G_0^{-1}(K) - G_0^{-1}(K+Q),
\tag{56}
$$

which can be shown to imply

$$
Q\cdot[\delta\Lambda_{AL_1}(K,K+Q) + \delta\Lambda_{MT}(K,K+Q)] = 0
\tag{57}
$$

so that $\delta\Lambda_{AL_1}(K,K)=-\delta\Lambda_{MT}(K,K)$ is obtained exactly from the $Q\to 0$ limit of the GWI.

To see this explicitly note that

$$
\begin{aligned}
\delta\Lambda^\mu_{MT} = -\sum_P & t(P)G_0(-K-Q+P) \\
&\times \lambda^\mu(-K-Q+P,-K+P) \\
&\times G_0(-K+P).
\end{aligned}
\tag{58}
$$

Similarly we have

$$
\begin{aligned}
\delta\Lambda^\mu_{AL_1} = -\sum_P & G_0(-K+P)t(P+Q) \\
&\times \left\{\sum_{K'} G(-K'+P)G_0(K'+Q)\right. \\
&\left.\times \lambda_\mu(K'+Q,K')G_0(K')\right\} t(P).
\end{aligned}
\tag{59}
$$

We may write

$$
t(P)^{-1} = U^{-1} - \sum_{K_1} G(K_1+P)G_0(-K_1).
\tag{60}
$$

Then combining terms

$$
\begin{aligned}
Q\cdot(\delta\Lambda_{MT}+\delta\Lambda_{AL_1}) = \sum_P & t(P)G_0(-K+P) \\
&\times \{G_0(-K-Q+P)[G_0^{-1}(P-K) \\
&- G_0^{-1}(P-K-Q)] - t(P+Q) \\
&\times \sum_{K'} G(-K'+P)G_0(K'+Q)G_0(K') \\
&\times [G_0^{-1}(K') - G_0^{-1}(K'+Q)]\}.
\end{aligned}
$$

It then follows using Eq. (60) that this equation vanishes and we have proved the desired relation between the Maki-Thompson vertex and the AL$_1$ vertex.

The GWI is *not* to be imposed on Λ since we are evaluating the electrodynamic response in a fixed (transverse) gauge. However, the full gauge covariant internal vertex Λ' is consistent with the GWI. This internal vertex Λ' then satisfies

$$Q \cdot \Lambda'(K,K+Q) = G^{-1}(K) - G^{-1}(K+Q). \qquad (61)$$

The above result can be used to infer a relation analogous to Eq. (57) for the AL_2 diagram: So that $\delta\Lambda_{AL_2}(K,K) = -\delta\Lambda_{MT}(K,K)$. More generally

$$Q \cdot (\delta\Lambda_{AL1} + \delta\Lambda_{AL2}) = -2Q \cdot \delta\Lambda_{MT}, \qquad (62)$$

Therefore, the combination of these three diagrams [in conjunction with Eq. (55)] leads to

$$Q \cdot \delta\Lambda_{pg}(K,K) = -Q \cdot \delta\Lambda_{MT}(K,K), \qquad (63)$$

which expresses this pseudogap contribution to the vertex entirely in terms of the Maki-Thompson diagram shown in the figure. One can show explicitly that

$$\delta\Lambda^{\mu}_{MT}(K,K) = -\frac{\partial\Sigma_{pg}(K)}{\partial k_\mu}. \qquad (64)$$

This can be proved as follows. We write

$$Q \cdot \delta\Lambda_{MT} = -\sum_P t_{pg}(P)[G_0(-K+P) - G_0(-K-Q+P)], \qquad (65)$$

where we have used the GWI involving the bare Green's functions to eliminate λ. Now taking the $\mathbf{q}=0$ limit with $\omega=0$ and using Eq. (63)) and the expression of $\Sigma_{pg}(K)$ we arrive at Eq. (64).

Combining terms we find

$$\delta\Lambda^{\mu}_{pg}(K,K) = \frac{\partial\Sigma_{pg}(K)}{\partial k_\mu}. \qquad (66)$$

This demonstrates consistency; that is, the usual Ward identity applies to the pseudogap contribution.

Now we turn to the superconducting vertex contributions. As can be seen by a simple inspection of the diagrams, the superconducting contribution is closely analogous to Eq. (64) so that we have

$$\delta\Lambda^{\mu}_{sc}(K,K) = -\frac{\partial\Sigma_{sc}(K)}{\partial k_\mu}. \qquad (67)$$

Importantly, the above equation contains a sign change [as compared with Eq. (66)]. This is associated with the transverse gauge and violates the Ward identity. It is central to the existence of a Meissner effect. The fact that the pseudogap contributions are consistent with generalized Ward identities is an important aspect of the present calculations. This implies that there is no direct Meissner contribution associated with the pseudogap self-energy.

We next explicitly evaluate the superfluid density using Eq. (50). For this purpose, we only need the spatial components of the vertex functions. Note that the pseudogap contribution to (n_s/m) drops out by virtue of Eq. (66). The density can be rewritten using integration by parts,

$$\left(\frac{n}{m}\right)_{\alpha\beta} = 2\sum_K \frac{\partial^2\epsilon_{\mathbf{k}}}{\partial k_\alpha \partial k_\beta} G(K) = -2\sum_K \frac{\partial\epsilon_{\mathbf{k}}}{\partial k_\alpha}\frac{\partial G(K)}{\partial k_\beta} = -2\sum_K G^2(K)\frac{\partial\epsilon_{\mathbf{k}}}{\partial k_\alpha}\left(\frac{\partial\epsilon_{\mathbf{k}}}{\partial k_\beta} + \frac{\partial\Sigma_{pg}}{\partial k_\beta} + \frac{\partial\Sigma_{sc}}{\partial k_\beta}\right), \qquad (68)$$

where $\alpha,\beta=1,2,3$. Note here the surface term vanishes in all cases. The superfluid density is given by

$$\frac{n_s}{m} = 2\sum_K G^2(K)\frac{\partial\epsilon_{\mathbf{k}}}{\partial k_x}\left[\delta\Lambda_{sc}(K,K)_x - \frac{\partial\Sigma_{sc}(K)}{\partial k_x}\right]. \qquad (69)$$

Equation (69) can be readily evaluated using the superconducting vertex and the superconducting self-energy $\Sigma_{sc}(K) = -\Delta_{sc}^2 G_0(-K)$ associated with our GG_0-based T-matrix approach. In addition, we introduce an approximation in our evaluation of G via Eq. (18) to find

$$\left(\frac{n_s}{m}\right) = 2\sum_{\mathbf{k}} \frac{\Delta_{sc}^2}{E_{\mathbf{k}}^2}\left[\frac{1-2f(E_{\mathbf{k}})}{2E_{\mathbf{k}}} + f'(E_{\mathbf{k}})\right]\left(\frac{\partial\epsilon_{\mathbf{k}}}{\partial k_x}\right)^2. \qquad (70)$$

More generally, we can define a relationship

$$\left(\frac{n_s}{m}\right) = \frac{\Delta_{sc}^2}{\Delta^2}\left(\frac{n_s}{m}\right)^{BCS}, \qquad (71)$$

where $(n_s/m)^{BCS}$ is just (n_s/m) with the overall prefactor Δ_{sc}^2 replaced with Δ^2 in Eq. (70). Obviously, in the pseudogap phase, $(n_s/m)^{BCS}$ does not vanish at T_c.

Finally, in the polarized case it can be shown that the superfluid density is given by Eq. (70) with the Fermi function and its derivative replaced by the quantities $\bar{f}$ and $\bar{f}'$, respectively.

A. Numerical results for unpolarized and polarized cases

The behavior of the superfluid density $n_s(T)$ is viewed as one of the important indicators of the quality of a given BCS-BEC crossover theory. Plots of $n_s(T)$ in Ref. 110 stop at about $T_c/2$, above which it is argued that the calculations are unreliable. Griffin and coworkers[111] have found double-valued functions, particularly on the BEC side of resonance. While $n_s(T)$ is not explicitly evaluated, it will necessarily exhibit a first order transition in the work of Ref. 64.

It is important, then, to show that $n_s(T)$ corresponds to the appropriate physical behavior in the current theory. First, we present results for unpolarized Fermi gases. The spatial distributions of $n_s(r)$ in a trap are plotted in Fig. 15 for different temperatures and three different scattering lengths ranging from near BCS to unitary to near BEC. In the insets are plotted the temperature dependence of the trap integrated superfluid density. All curves are well behaved, single-valued, and monotonic from $T=0$ to $T=T_c$. The superfluid density vanishes precisely at T_c.

Analogous plots are shown in Fig. 16 for a polarized gas in the unitary case and at three different polarizations $\delta=0.1$, 0.5, and 0.8. The main figures present plots as a function of trap radius, whereas the insets are plots as a function of temperature. Here, by contrast, the behavior is *not* always smooth. These sharp features are all expected and associated

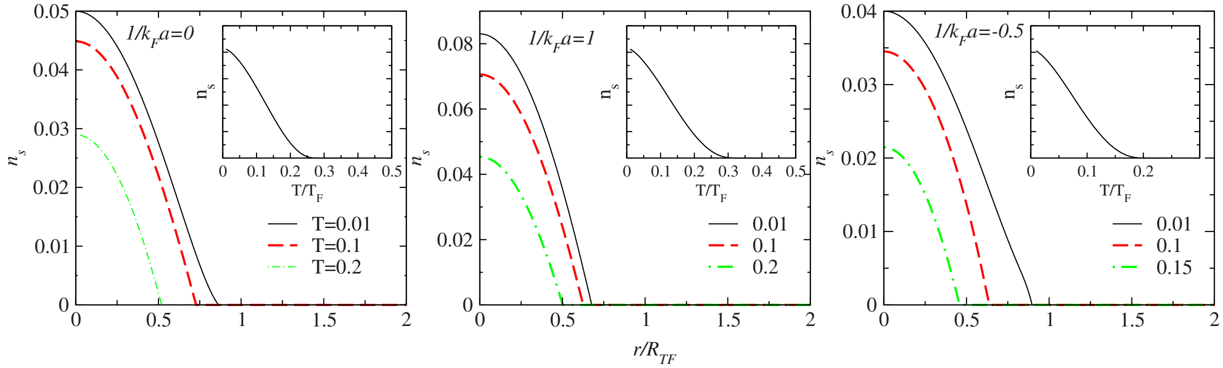

FIG. 15. (Color online) Spatial profiles of superfluid density at zero polarization at different temperatures (as labeled) for $1/k_Fa=0$ (left), 1 (middle), and −0.5 (right panel). The insets show the T dependence of trap integrated superfluid density. All the profiles are smooth, single-valued, and monotonic, evolving continuously with radius and temperature.

strictly with polarization effects. Importantly, they disappear in the absence of polarization. At the lowest temperatures in the main body of each of these figures one can see the effects of phase separation on n_s. The superfluid density stops abruptly at the interface between the normal and superfluid. At higher T in the Sarma phase, the curves end continuously at the trap edge. At the higher two polarizations the two insets indicate kinks which reflect the transition from a phase separated to a Sarma phase.

IX. CONCLUSIONS

There are many different versions of BCS-BEC crossover physics in the literature, but what has guided us here is the implementation of a sound methodology for characterizing three fundamental properties: Thermodynamics, density profiles and superfluid density with and without population imbalance. While there is considerable emphasis in the literature on numerical precision one goal of this paper was to set up a different set of criteria against which theories as well as simulations can be measured. Monte Carlo simulations are sometimes argued[112] to be the ultimate theory. While they may provide reliable numbers, these alone (in the absence of more analytic many body schemes) will not yield sufficient insight into the complex physics of these very anomalous superfluids.

Four important and inter-related physical properties were emphasized here. (i) There must be a self-consistent treatment of "pseudogap" effects. That is, the fermionic excitation spectrum, $E_{\mathbf{k}}$, must necessarily be different from the usual BCS form (which is presumed in all other theories of crossover and in which there is a pairing gap which vanishes in the normal state). Here, based on a systematic analysis, we show that, for our particular T-matrix theory, the BCS form for $E_{\mathbf{k}}$ is maintained naturally[74,75] but with an order parameter replaced by the total excitation gap Δ. (ii) The theory must lend itself to a consistent description of the superfluid density $n_s(T)$ from zero to T_c. The quantity $n_s(T)$ should be single valued and monotonic.[14] It must necessarily disappear at the same T_c one computes from the normal state instability; *$n_s(T)$ is at the heart of a proper description of the superfluid phase*. (iii) The behavior of the density profiles, which are at the basis for all thermodynamical calculations of trapped Fermi gases, must be compatible with experiment. Near and at unitarity, in an unpolarized gas, they are relatively smooth and featureless, well fit to a Thomas-Fermi–like form. Only in the presence of polarization effects can

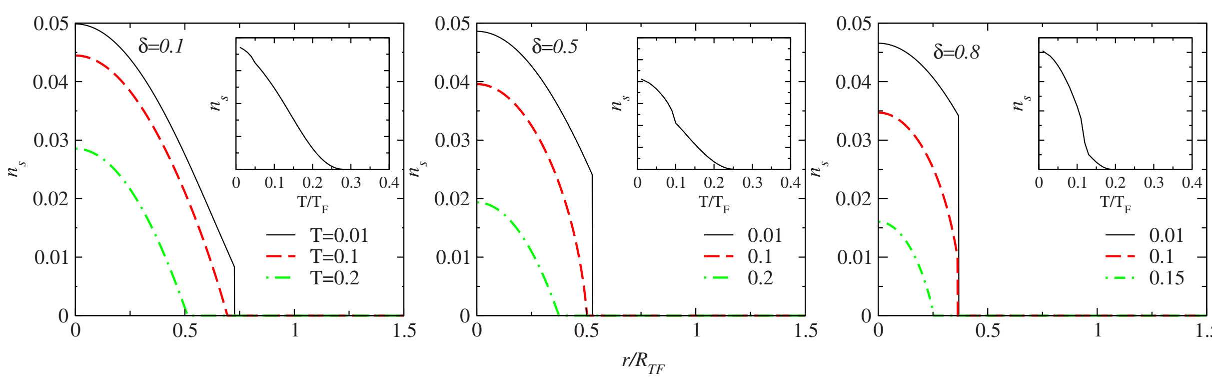

FIG. 16. (Color online) Spatial profiles of superfluid density at unitary at different temperatures (as labeled) for polarization δ=0.1, 0.5, and 0.8 from left to right. The insets show the trap integrated superfluid density as function of T. High T profiles are in the Sarma phase, and therefore, smooth, evolving continuously with radius. In contrast, the lowest T curves are in the phase separation regime and thus show a abrupt drop. The kinks in the trap integrated n_s reflect the transition from phase separation to Sarma state.

one use these unitary profiles to find signatures of the condensate edge. (iv) The thermodynamical potential Ω should be variationally consistent with both the gap and number equations. This condition is generally violated in all other pairing fluctuation theories (which are inconsistent because these fluctuations enter only into the number equation, but not the gap equation). In addition, Ω should satisfy appropriate Maxwell relations and at unitarity be compatible with the constraint relating the pressure p to the energy density: $p = \frac{2}{3}E$. Here we find this to be the case for a population imbalanced gas as well, at least at the same level of numerical precision as for an unpolarized gas.

For semiquantitative comparisons with experiment there have been notable successes within the present theoretical framework which address a very wide group of experiments, including polarized and unpolarized gases.[4,46–49,88,96,113,114] However, it is clear that detailed quantitative agreement is not always possible.[115] The calculated β factor at unitarity ($\beta = -0.41$), is not precise, as compared with experiment ($\beta \approx -0.55$). Moreover, the ratio of effective interboson scattering length to the fermionic scattering length is found to be 2.0, rather than 0.6.[69] Indeed, interboson effects are included only in a mean field sense at the level of the simple BCS-Leggett wave function and related T-matrix scheme. One knows[19] how to arrive at a more Bogoliubov-like treatment of the pairs which properly treats inter-boson effects appropriate to the deep BEC. It can be shown[19] to yield the factor 0.6. This involves adding to the wave function additional terms involving four and six creation operators. However, there is no natural and tractable extension at unitarity.

We have emphasized here that what is most unique and interesting about these trapped Fermi gases lies not so much in the ground state, but rather in finite temperature phenomena. It is at finite T that one sees a new form of fermionic superfluidity in which pair condensation and pair formation take place on distinctly different temperature scales. This temperature separation requires radical changes in the way we think about fermionic superfluidity, relative to our experience with strict BCS theory. We have argued here that at this relatively early stage of our understanding, it is more important to capture the central physics of this exotic superfluidity than to arrive at precise numerical agreement with experiment. Ultimately we must do both, as has been possible for the Bose gases. Nevertheless assessing a theory based on understanding the qualitative physics has to proceed an assessment based on quantitative comparisons.

Note added in proof. Recently, an experimental paper on the phase diagram of the homogenous system appeared.[116] A comparison of Fig. 4 and their Fig. 5 shows qualitatively similar features. However, unlike their Fig. 5, we do not find the phase boundaries to be straight lines.

ACKNOWLEDGMENTS

This work is supported by Grant Nos. NSF PHY-0555325 and NSF-MRSEC DMR-0213745.

[1] A. J. Leggett, Nat. Phys. **2**, 134 (2006).
[2] M. Randeria, in *Models and Phenomenology for Conventional and High-temperature Superconductivity*, Proceedings of the International School of Physics "Enrico Fermi" Courses, edited by G. Iadonisi, J. R. Schrieffer, and M. L. Chiafalo, Società Italiana di Fisica Bologna, Italy (IOS Press, 1998), Vol. 136, pp. 53–75. Here, however, it was incorrectly argued that for BCS-BEC crossover "there is no pseudogap in the charge channel."
[3] Q. J. Chen, J. Stajic, S. N. Tan, and K. Levin, Phys. Rep. **412**, 1 (2005).
[4] K. Levin and Q. J. Chen, arXiv:cond-mat/0610006 (unpublished).
[5] M. Greiner, C. A. Regal, and D. S. Jin, Nature (London) **426**, 537 (2003).
[6] S. Jochim, M. Bartenstein, A. Altmeyer, G. Hendl, S. Riedl, C. Chin, J. H. Denschlag, and R. Grimm, Science **302**, 2101 (2003).
[7] M. W. Zwierlein, C. A. Stan, C. H. Schunck, S. H. F. Raupach, S. Gupta, Z. Hadzibabic, and W. Ketterle, Phys. Rev. Lett. **91**, 250401 (2003).
[8] S. Giorgini, L. P. Pitaevskii, and S. Stringari, arXiv:0706.3360 (unpublished).
[9] D. M. Eagles, Phys. Rev. **186**, 456 (1969).
[10] A. J. Leggett, *Modern Trends in the Theory of Condensed Matter* (Springer-Verlag, Berlin, 1980), pp. 13–27.
[11] R. Micnas, J. Ranninger, and S. Robaszkiewicz, Rev. Mod. Phys. **62**, 113 (1990).
[12] M. Randeria, in *Bose Einstein Condensation*, edited by A. Griffin, D. Snoke, and S. Stringari (Cambridge University Press, Cambridge, UK, 1995), pp. 355–92.
[13] P. Pieri and G. C. Strinati, Phys. Rev. B **71**, 094520 (2005).
[14] To be precise, for a homogeneous Fermi gas with population imbalance, the superfluid density has been found to exhibit a nonmonotonic dependence on temperature in the unitary and BCS regimes. This leads to intermediate temperature superfluidity (Refs. 84 and 85). Nevertheless, it has been found to be monotonic in a trap.
[15] T.-L. Ho, Phys. Rev. Lett. **92**, 090402 (2004).
[16] J. E. Thomas, J. Kinast, and A. Turlapov, Phys. Rev. Lett. **95**, 120402 (2005).
[17] P. Nozières and S. Schmitt-Rink, J. Low Temp. Phys. **59**, 195 (1985).
[18] I. Kosztin, Q. J. Chen, Y.-J. Kao, and K. Levin, Phys. Rev. B **61**, 11662 (2000).
[19] S. N. Tan and K. Levin, Phys. Rev. A **74**, 043606 (2006).
[20] P. Pieri and G. C. Strinati, Phys. Rev. Lett. **91**, 030401 (2003).
[21] K. Machida, T. Mizushima, and M. Ichioka, Phys. Rev. Lett. **97**, 120407 (2006).
[22] J. Kinnunen, L. M. Jensen, and P. Törmä, Phys. Rev. Lett. **96**, 110403 (2006); L. M. Jensen, J. Kinnunen, and P. Törmä, Phys. Rev. A **76**, 033620 (2007); T. Mizushima, K. Machida, and M. Ichioka, Phys. Rev. Lett. **94**, 060404 (2005); T. Mizushima, M. Ichioka, and K. Machida, J. Phys. Soc. Jpn. **76**, 104006 (2007); R. Sensarma, W. Schneider, R. B. Diener, and M. Randeria, arXiv:0706.1741 (unpublished).

[23] Q. J. Chen, Y. He, C.-C. Chien, and K. Levin, Phys. Rev. B **75**, 014521 (2007).
[24] Q. J. Chen, I. Kosztin, B. Jankó, and K. Levin, Phys. Rev. Lett. **81**, 4708 (1998).
[25] R. Micnas and S. Robaszkiewicz, Condens. Matter Phys. **1**, 89 (1998).
[26] J. Ranninger and J. M. Robin, Phys. Rev. B **53**, R11961 (1996).
[27] A. Perali, P. Pieri, G. C. Strinati, and C. Castellani, Phys. Rev. B **66**, 024510 (2002).
[28] J. N. Milstein, S. J. J. M. F. Kokkelmans, and M. J. Holland, Phys. Rev. A **66**, 043604 (2002).
[29] Y. Ohashi and A. Griffin, Phys. Rev. Lett. **89**, 130402 (2002).
[30] Y. Ohashi and A. Griffin, Phys. Rev. A **67**, 063612 (2003).
[31] P. Pieri, L. Pisani, and G. C. Strinati, Phys. Rev. Lett. **92**, 110401 (2004).
[32] N. Trivedi and M. Randeria, Phys. Rev. Lett. **75**, 312 (1995).
[33] B. Jankó, J. Maly, and K. Levin, Phys. Rev. B **56**, R11407 (1997).
[34] Q. J. Chen, K. Levin, and I. Kosztin, Phys. Rev. B **63**, 184519 (2001).
[35] Q. J. Chen, I. Kosztin, B. Jankó, and K. Levin, Phys. Rev. Lett. **81**, 4708 (1998).
[36] J. M. Singer, M. H. Pedersen, and T. Schneider, Physica B **230**, 955 (1997).
[37] M. H. Pedersen, J. J. Rodriguez-Nunez, H. Beck, T. Schneider, and S. Schafroth, Z. Phys. B: Condens. Matter **103**, 21 (1997).
[38] Q. J. Chen, I. Kosztin, B. Jankó, and K. Levin, Phys. Rev. B **59**, 7083 (1999).
[39] J. C. Campuzano, M. R. Norman, and M. Randeria, in *Physics of Superconductors*, edited by K. H. Bennemann and J. B. Ketterson (Springer-Verlag, Berlin, 2004), Vol. II, pp. 167–273.
[40] A. G. Loeser, Z.-X. Shen, D. S. Dessau, D. S. Marshall, C. H. Park, P. Fournier, and A. Kapitulnik, Science **273**, 325 (1996).
[41] To be precise, the symmetry for the pseudogap is $|d_{x^2-y^2}|$, which does not have a sign change.
[42] J. Stajic, J. N. Milstein, Q. J. Chen, M. L. Chiofalo, M. J. Holland, and K. Levin, Phys. Rev. A **69**, 063610 (2004).
[43] A. Perali, P. Pieri, L. Pisani, and G. C. Strinati, Phys. Rev. Lett. **92**, 220404 (2004).
[44] C. Chin, M. Bartenstein, A. Altmeyer, S. Riedl, S. Jochim, J. Hecker-Denschlag, and R. Grimm, Science **305**, 1128 (2004).
[45] J. Kinnunen, M. Rodriguez, and P. Törmä, Phys. Rev. Lett. **92**, 230403 (2004).
[46] J. Kinnunen, M. Rodriguez, and P. Törmä, Science **305**, 1131 (2004).
[47] Y. He, Q. J. Chen, and K. Levin, Phys. Rev. A **72**, 011602(R) (2005).
[48] J. Kinast, A. Turlapov, J. E. Thomas, Q. J. Chen, J. Stajic, and K. Levin, Science **307**, 1296 (2005).
[49] W. Yi and L. M. Duan, Phys. Rev. A **73**, 031604(R) (2006).
[50] P. Castorina, M. Grasso, M. Oertel, M. Urban, and D. Zappalà, Phys. Rev. A **72**, 025601 (2005).
[51] P. Fulde and R. A. Ferrell, Phys. Rev. **135**, A550 (1964); A. I. Larkin and Y. N. Ovchinnikov, Zh. Eksp. Teor. Fiz. **47**, 1136 (1964) [Sov. Phys. JETP **20**, 762 (1965)].
[52] Y. Shin, M. W. Zwierlein, C. H. Schunck, A. Schirotzek, and W. Ketterle, Phys. Rev. Lett. **97**, 030401 (2006).
[53] G. B. Partridge, W. Li, R. I. Kamar, Y. A. Liao, and R. G. Hulet, Science **311**, 503 (2006).
[54] Y. He, C.-C. Chien, Q. J. Chen, and K. Levin, Phys. Rev. A **75**, 021602(R) (2007).
[55] L. P. Kadanoff and P. C. Martin, Phys. Rev. **124**, 670 (1961).
[56] Q. J. Chen, Ph.D. thesis, University of Chicago, 2000 (available in the ProQuest Dissertations & Theses Database online).
[57] A. L. Fetter and J. D. Walecka, *Quantum Theory of Many-Particle Systems* (McGraw-Hill, San Francisco, 1971).
[58] R. Haussmann, Z. Phys. B: Condens. Matter **91**, 291 (1993).
[59] N. E. Bickers, D. J. Scalapino, and S. R. White, Phys. Rev. Lett. **62**, 961 (1989); N. E. Bickers and D. J. Scalapino, Ann. Phys. (N.Y.) **193**, 206 (1989).
[60] J. J. Deisz, D. W. Hess, and J. W. Serene, Phys. Rev. Lett. **76**, 1312 (1996).
[61] G. Baym, Phys. Rev. **127**, 1391 (1962).
[62] Y. M. Vilk and A. M. S. Tremblay, J. Phys. I **7**, 1309 (1997).
[63] O. Tchernyshyov, Phys. Rev. B **56**, 3372 (1997).
[64] R. Haussmann, W. Rantner, S. Cerrito, and W. Zwerger, Phys. Rev. A **75**, 023610 (2007).
[65] J. W. Serene, Phys. Rev. B **40**, 10873 (1989).
[66] H. Hu, X. J. Liu, and P. D. Drummond, Phys. Rev. A **73**, 023617 (2006); Europhys. Lett. **74**, 574 (2006).
[67] These same authors recently investigated an approach which uses a mix of G_0 and G in the T matrix and obtained different results from the present work. It should be pointed out that they failed to include the noncondensed pair contribution in the gap equation.
[68] A. Perali, P. Pieri, and G. C. Strinati, Phys. Rev. Lett. **93**, 100404 (2004).
[69] D. S. Petrov, C. Salomon, and G. V. Shlyapnikov, Phys. Rev. Lett. **93**, 090404 (2004).
[70] P. Pieri and G. C. Strinati, Phys. Rev. Lett. **96**, 150404 (2006).
[71] I. V. Brodsky, M. Y. Kagan, A. V. Klaptsov, R. Combescot, and X. Leyronas, Phys. Rev. A **73**, 032724 (2006).
[72] J. Levinsen and V. Gurarie, Phys. Rev. A **73**, 053607 (2006).
[73] B. R. Patton, Ph.D. thesis, Cornell University, 1971.
[74] J. Maly, B. Jankó, and K. Levin, Physica C **321**, 113 (1999).
[75] I. Kosztin, Q. J. Chen, B. Jankó, and K. Levin, Phys. Rev. B **58**, R5936 (1998).
[76] C.-C. Chien, Q. J. Chen, Y. He, and K. Levin, Phys. Rev. A **74**, 021602(R) (2006).
[77] G. B. Partridge, W. H. Li, Y. A. Liao, R. G. Hulet, M. Haque, and H. T. C. Stoof, Phys. Rev. Lett. **97**, 190407 (2006).
[78] G. Sarma, J. Phys. Chem. Solids **24**, 1029 (1963).
[79] M. M. Forbes, E. Gubankova, W. V. Liu, and F. Wilczek, Phys. Rev. Lett. **94**, 017001 (2005).
[80] C. H. Pao, S. T. Wu, and S. K. Yip, Phys. Rev. B **73**, 132506 (2006).
[81] D. E. Sheehy and L. Radzihovsky, Phys. Rev. Lett. **96**, 060401 (2006).
[82] T. N. De Silva and E. J. Mueller, Phys. Rev. Lett. **97**, 070402 (2006).
[83] M. Haque and H. T. C. Stoof, Phys. Rev. A **74**, 011602(R) (2006).
[84] C.-C. Chien, Q. J. Chen, Y. He, and K. Levin, Phys. Rev. Lett. **97**, 090402 (2006).
[85] Q. J. Chen, Y. He, C.-C. Chien, and K. Levin, Phys. Rev. A **74**, 063603 (2006).
[86] M. M. Parish, F. M. Marchetti, A. Lamacraft, and B. D. Simons, Nat. Phys. **3**, 124 (2007).
[87] P. F. Bedaque, H. Caldas, and G. Rupak, Phys. Rev. Lett. **91**, 247002 (2003); H. Caldas, Phys. Rev. A **69**, 063602 (2004).

[88] C.-C. Chien, Q. J. Chen, Y. He, and K. Levin, Phys. Rev. Lett. **98**, 110404 (2007).

[89] J. Maly, B. Jankó, and K. Levin, Phys. Rev. B **59**, 1354 (1999).

[90] A. Imambekov, C. J. Bolech, M. Lukin, and E. Demler, Phys. Rev. A **74**, 053626 (2006).

[91] K. M. O'Hara, S. L. Hemmer, M. E. Gehm, S. R. Granade, and J. E. Thomas, Science **298**, 2179 (2002).

[92] M. Bartenstein, A. Altmeyer, S. Riedl, S. Jochim, C. Chin, J. H. Denschlag, and R. Grimm, Phys. Rev. Lett. **92**, 120401 (2004).

[93] J. Kinast, A. Turlapov, and J. E. Thomas, arXiv:cond-mat/0409283 (unpublished).

[94] M. L. Chiofalo, S. J. J. M. F. Kokkelmans, J. N. Milstein, and M. J. Holland, Phys. Rev. Lett. **88**, 090402 (2002).

[95] X.-J. Liu, H. Hu, and P. D. Drummond, Phys. Rev. A **75**, 023614 (2007).

[96] J. Stajic, Q. J. Chen, and K. Levin, Phys. Rev. Lett. **94**, 060401 (2005).

[97] T. N. De Silva and E. J. Mueller, Phys. Rev. A **73**, 051602(R) (2006).

[98] It should be noted that, within the local density approximation, the spatial gradient term is absent in the thermodynamic potential. Such a term may have a slight quantitative effect on the boundary between the phase-separated phase and its neighboring phases.

[99] M. W. Zwierlein, A. Schirotzek, C. H. Schunck, and W. Ketterle, Science **311**, 492 (2006).

[100] M. W. Zwierlein, C. H. Schunck, A. Schirotzek, and W. Ketterle, Nature (London) **442**, 54 (2006).

[101] Q. J. Chen, J. Stajic, and K. Levin, Phys. Rev. Lett. **95**, 260405 (2005).

[102] M. Greiner, C. A. Regal, and D. S. Jin, Phys. Rev. Lett. **94**, 070403 (2005).

[103] Q. J. Chen, I. Kosztin, and K. Levin, Phys. Rev. Lett. **85**, 2801 (2000).

[104] G. D. Mahan, *Many-Particle Physics*, 2nd ed. (Plenum Press, New York, 1990).

[105] A. J. Leggett, Phys. Rev. **140**, A1869 (1965).

[106] A. J. Leggett, in *Low Temperature Physics*, edited by M. J. Hoch, D. Ruelle, R. L. Jaffe, J. Ehlers, and K. Hepp, Lecture Notes in Physics, Vol. 394 (Springer, Berlin/Heidelberg, 1991), pp. 1–92.

[107] R. Combescot, J. Low Temp. Phys. **18**, 537 (1975).

[108] M. C. Cross, J. Low Temp. Phys. **21**, 525 (1975).

[109] P. W. Anderson and W. F. Brinkman, in *The Physics of Superfluid and Solid Helium - Part II*, edited by K. H. Bennemann and J. B. Ketterson, Interscience Monographs & Texts in Physics & Astronomy, Vol. 29 (John Wiley & Sons, Inc., New York, Chichester, Brisbane, Toronto, 1978), Chap. 3, pp. 177–286.

[110] N. Andrenacci, P. Pieri, and G. C. Strinati, Phys. Rev. B **68**, 144507 (2003).

[111] E. Taylor, A. Griffin, N. Fukushima, and Y. Ohashi, Phys. Rev. A **74**, 063626 (2006); N. Fukushima, Y. Ohashi, E. Taylor, and A. Griffin, *ibid.* **75**, 033609 (2007).

[112] A. Bulgac, J. E. Drut, and P. Magierski, Phys. Rev. Lett. **96**, 090404 (2006).

[113] Q. J. Chen, C. A. Regal, M. Greiner, D. S. Jin, and K. Levin, Phys. Rev. A **73**, 041601(R) (2006).

[114] Q. J. Chen, C. A. Regal, D. S. Jin, and K. Levin, Phys. Rev. A **74**, 011601(R) (2006).

[115] A. Altmeyer, S. Riedl, C. Kohstall, M. J. Wright, R. Geursen, M. Bartenstein, C. Chin, J. H. Denschlag, and R. Grimm, Phys. Rev. Lett. **98**, 040401 (2007).

[116] Y. Shin, C. H. Schunck, A. Schirotzek, and W. Ketterle, arXiv:0709.3027 (unpublished).